Simuler les Propriétés *Mécaniques* des *Verres,* et des matériaux *désordonnés.*

A.Tanguy

http://www-lpmcn.univ-lyon1.fr/~atanguy

Laboratoire LPMCN
Theory Group
Université Claude Bernard – Lyon 1
(France)

T. Albaret, J.-L. Barrat, C. Fusco, C. Goldenberg, G. Kermouche,
F. Léonforte, B. Mantisi, A. Mokshin, M. Talati, M. Tsamados, J.P. Wittmer

I. **Systems and Simulations**
examples of amorphous materials
Molecular Dynamics Simulations
Energy Minimization
Mesoscopic Modelling

II. **Statistical Analysis**
local dynamics
correlated motion

III. **Computation of Mechanical Quantities**
stress, strain, Elastic Moduli
identification of plastic rearrangements

I. Systems and Simulations

examples of amorphous materials
Molecular Dynamics Simulations
Energy Minimization
Mesoscopic Modelling

Examples of *amorphous* materials

Covalent glasses:
a-Si, silica…

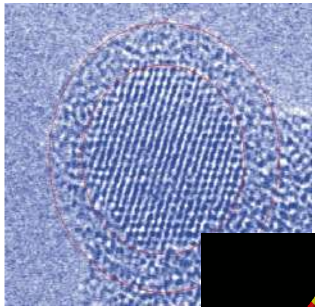

Si PCML –université Lyon I

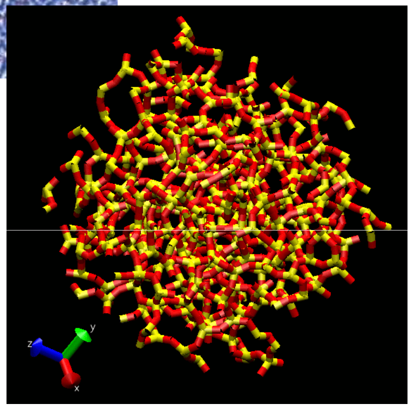

SiO_2, F. Léonforte

Metallic glasses:
Zr-Ti-Cu-Ni-Be, Mg-Cu-Y,
Fe-B…

Metallic glasses, Vitreloy

Polymeric glasses:
PMMA,PC, PS…

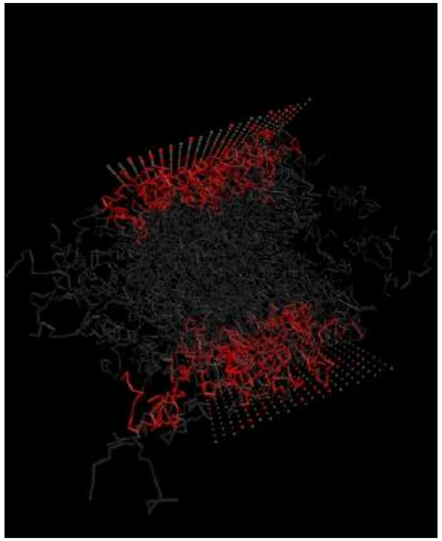

Disordered dense assemblies:
Foams, cells,…

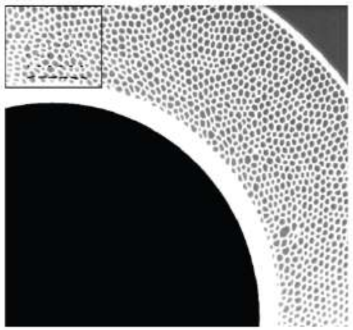

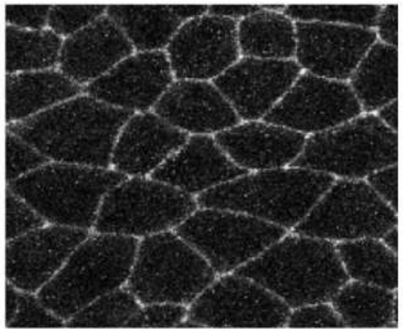

Granular media

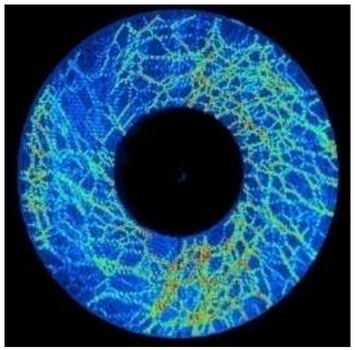

Colloïds

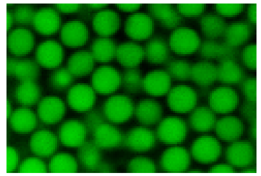

Colloids: 2 micron diameters
3D confocal microscopy.
E.R. Weeks (2006)

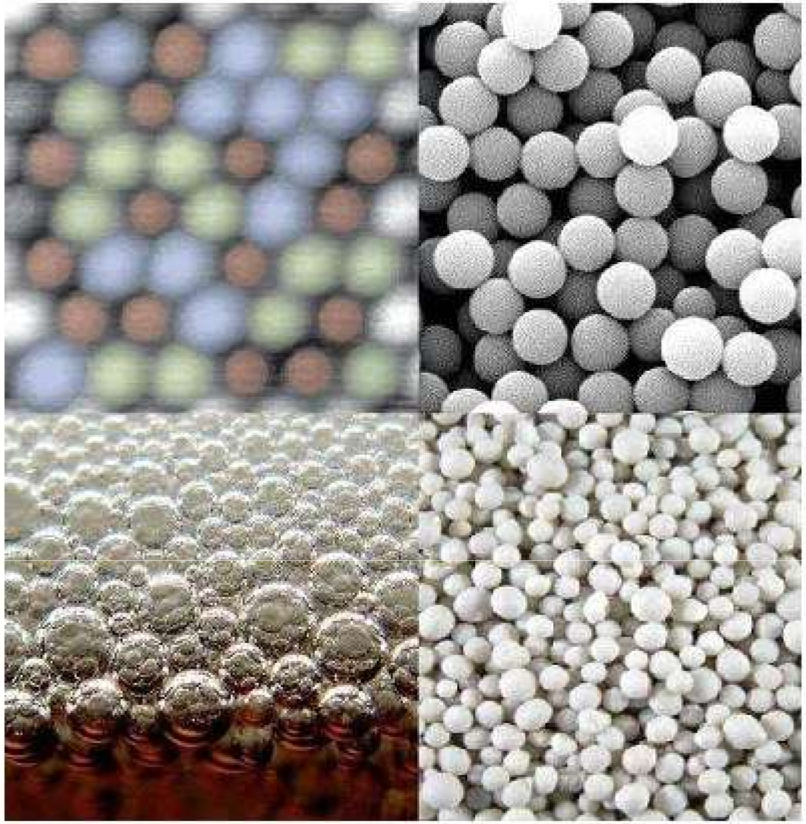

FIG. 1 Glassy phases occur at low temperature or large density in many different systems spanning a broad range of lengthscales, such as atomic (top left, atomic force spectroscopy image of an alloy linear size 4.3 nm (Sugimoto *et al.*, 2007)), colloidal (top right) systems, foams (bottom left, a beer foam with bubbles of submillimeter size) and granular materials (bottom right, a fertilizer made of millimeter size grains).

L. Berthier (2010)

Classical Simulations on different systems

The crucial choice of the **empirical** interactions

Examples:

Lennard-Jones Glasses

N = 100 to 400 000 particles
L: 10 a to 630 a (2D)
5 a to 74 a (3D)
ρ: 0.87 to 1.4

Amorphous « silicon »

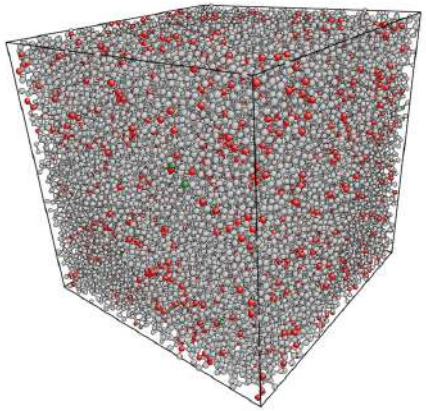

N = 32 768 atoms
L = 84.8 Å
ρ = 2.4 g/cm^3

Silica glass

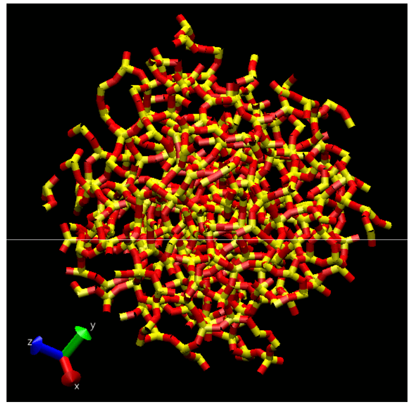

N = 3 000 to 192 000 atoms
L = 36 to 143 Å
ρ= 2.2 to 3 g/cm^3

$$V_{ij}(r) = 4\epsilon_{ij}\left\{\left(\frac{\sigma_{ij}}{r}\right)^{12} - \left(\frac{\sigma_{ij}}{r}\right)^{6}\right\}$$

$$E_{SW} = \Sigma_{i,j}(A.r_{ij}^{-4} - B).e^{(r_{ij}-a)^{-1}} + \Sigma_{i,j,k}\lambda.(\cos\theta_{jik} + 1/3)^2.e^{\gamma.(r_{ij}-a)^{-1}+\gamma.(r_{ik}-a)^{-1}}$$

$$E_{BKS}(r) = \frac{q_i q_j}{4\pi\varepsilon_0 r} + A_{ij}e^{-B_{ij}r} - \frac{C_{ij}}{r^6}$$

with $(i, j) \in \{Si, O\}$

	Short-range parameters			Atomic charges
i-j	A_{ij} (eV)	b_{ij} (Å^{-1})	c_{ij} (eV Å^6)	
O-O	1388.7730	2.76000	175.0000	$q_O = -1.2$
Si-O	18003.7572	4.87318	133.5381	$q_{Si} = 2.4$

Measuring Systems - Geometries

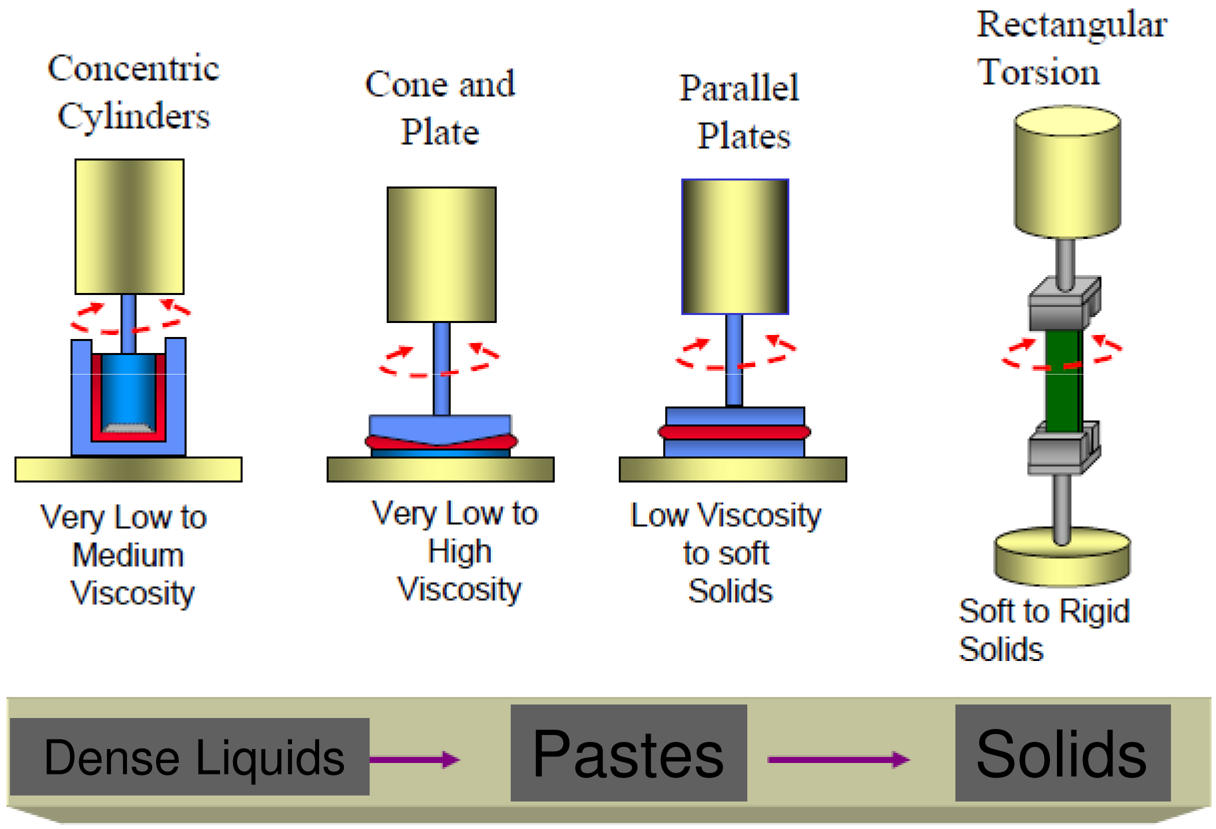

Example: Elasto-Plastic Mechanical Response

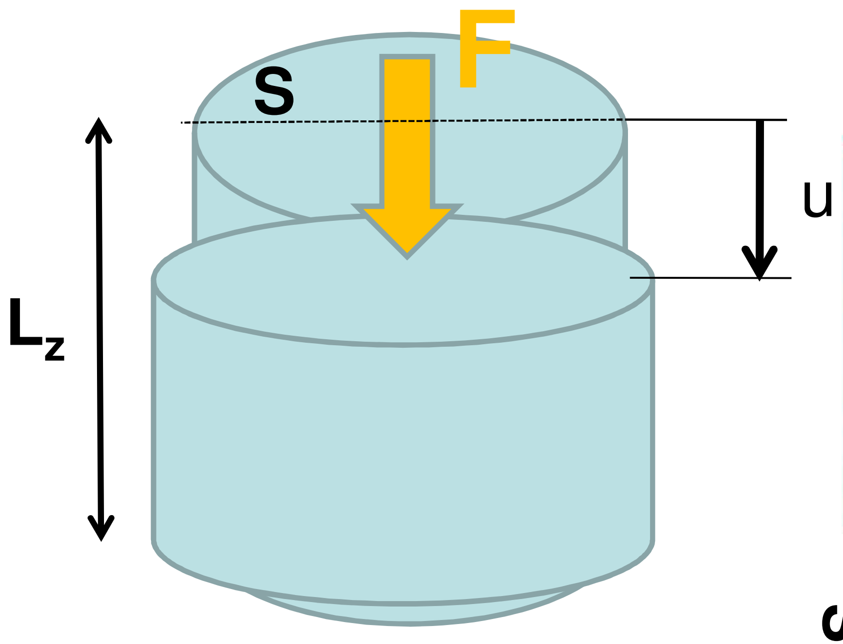

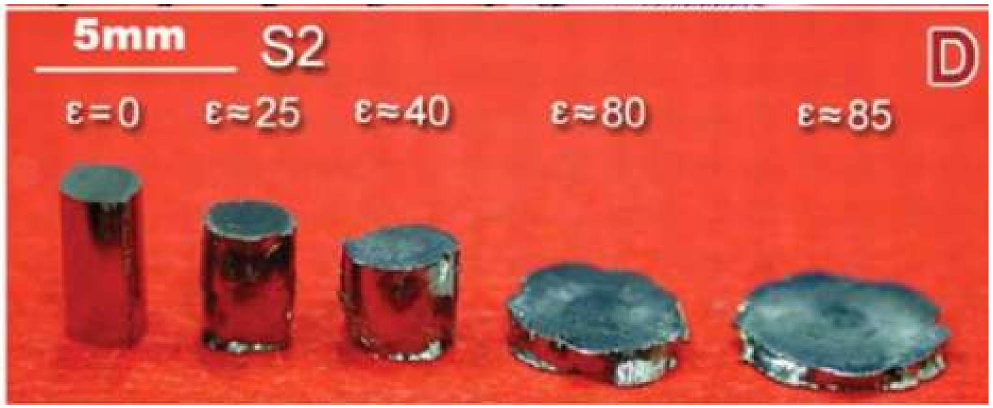

vitreloy

Linear Response:

$F/S = \mathbf{E}.u/L_z$

stress σ

elastic modulus

strain ε

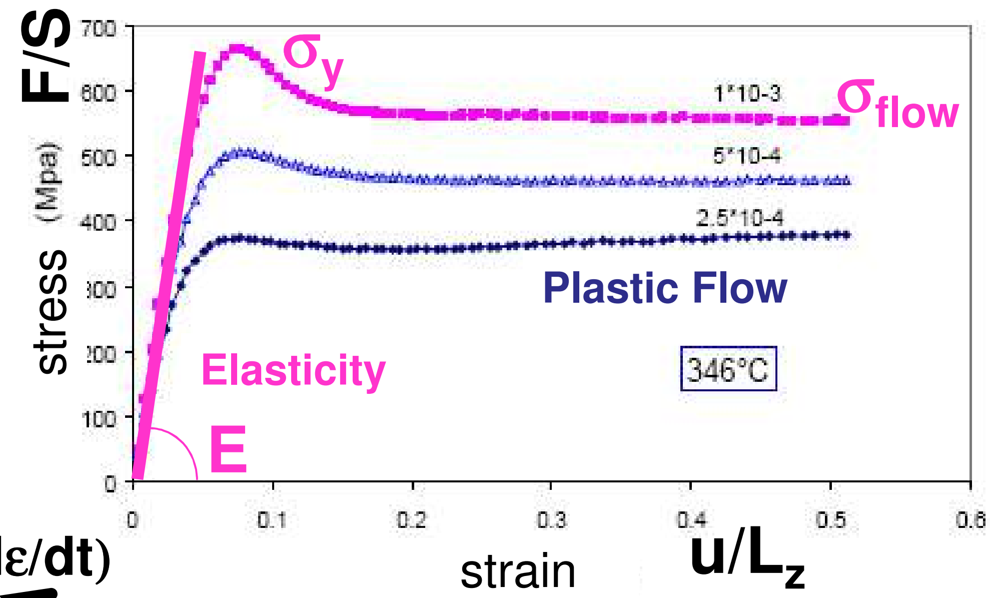

Yield stress σ_y

Visco-Plastic Flow stress σ_{flow} ($d\varepsilon/dt$)

Strain rate $d\varepsilon/dt$

Specific Mechanical Properties:

Elastic Moduli:

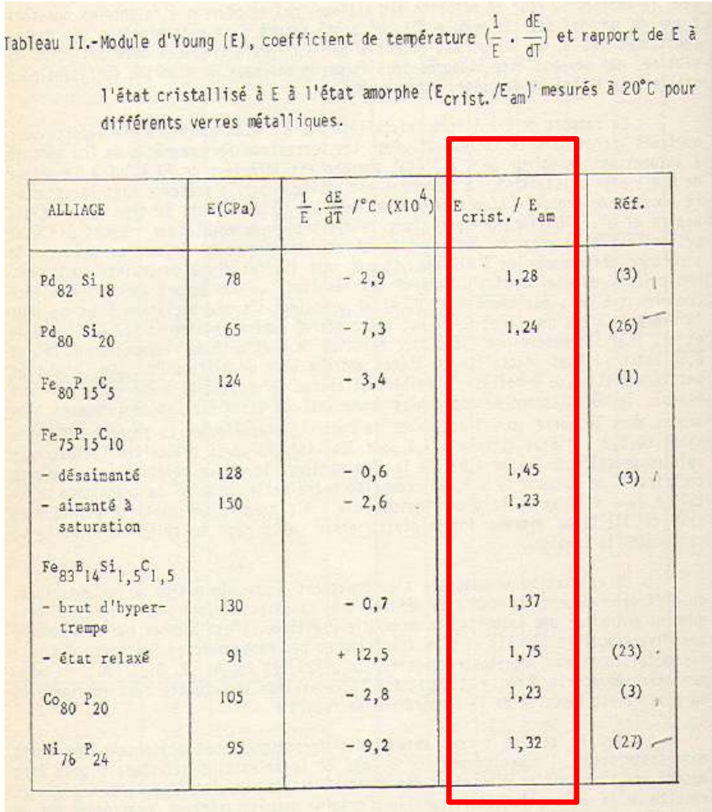

Tableau II.-Module d'Young (E), coefficient de température ($\frac{1}{E} \cdot \frac{dE}{dT}$) et rapport de E à l'état cristallisé à E à l'état amorphe ($E_{crist.}/E_{am}$) mesurés à 20°C pour différents verres métalliques.

ALLIAGE	E(GPa)	$\frac{1}{E}\cdot\frac{dE}{dT}$ /°C (x10^4)	$E_{crist.}$ / E_{am}	Réf.
$Pd_{82}Si_{18}$	78	- 2,9	1,28	(3)
$Pd_{80}Si_{20}$	65	- 7,3	1,24	(26)
$Fe_{80}P_{15}C_5$	124	- 3,4		(1)
$Fe_{75}P_{15}C_{10}$				
- désaimanté	128	- 0,6	1,45	(3)
- aimanté à saturation	150	- 2,6	1,23	
$Fe_{83}B_{14}Si_{1,5}C_{1,5}$				
- brut d'hyper-trempe	130	- 0,7	1,37	
- état relaxé	91	+ 12,5	1,75	(23)
$Co_{80}P_{20}$	105	- 2,8	1,23	(3)
$Ni_{76}P_{24}$	95	- 9,2	1,32	(27)

$E_{amorphous} \approx E_{crist.} / 1.3 < E_{crist}$

Very high Elastic Limit:

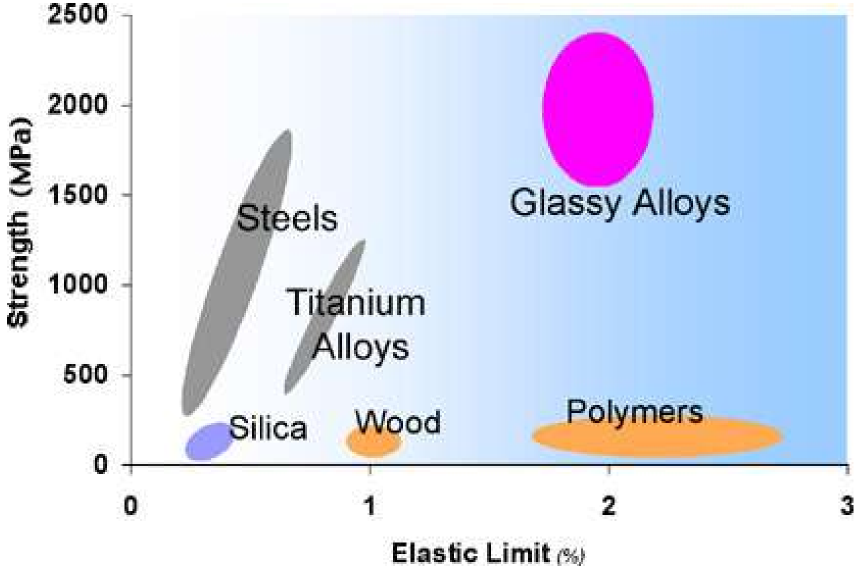

Strain Localization along shear bands:

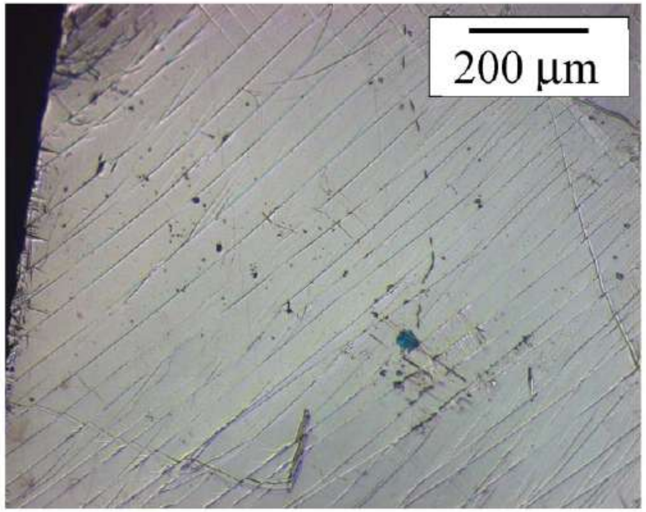

Scroers et Johnson (2004)

$Pt_{57.5}Cu_{14.7}Ni_{5.3}P_{22.5}$

« Anormalous » density of Low ω Vibration Modes:

Boson Peak

$$\frac{g(\omega)}{\omega^2} \propto \frac{g(\omega)}{g_D(\omega)}$$

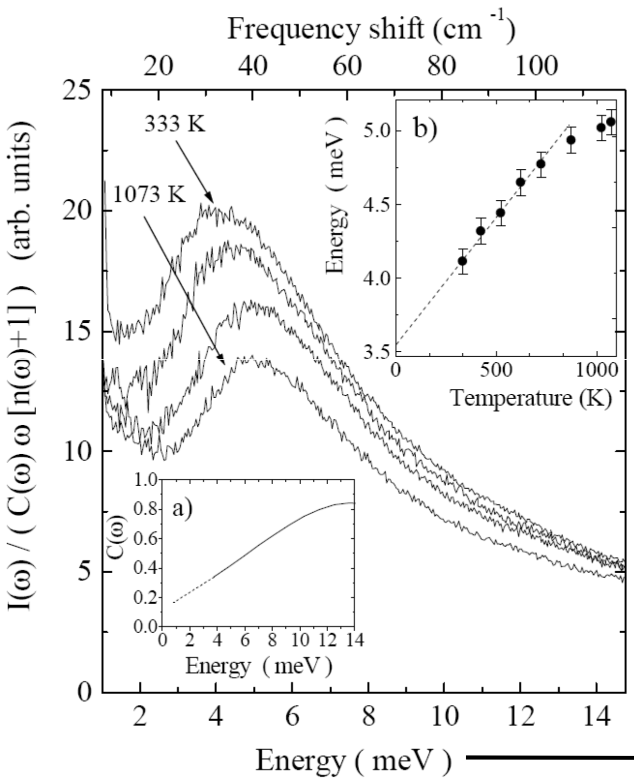

ω

Raman Specra of a-SiO2
by C. Masciovecchio et al.(1999)

High Heat Capacity:

$$\delta Q = C_v . dT$$

(density of vibrations)

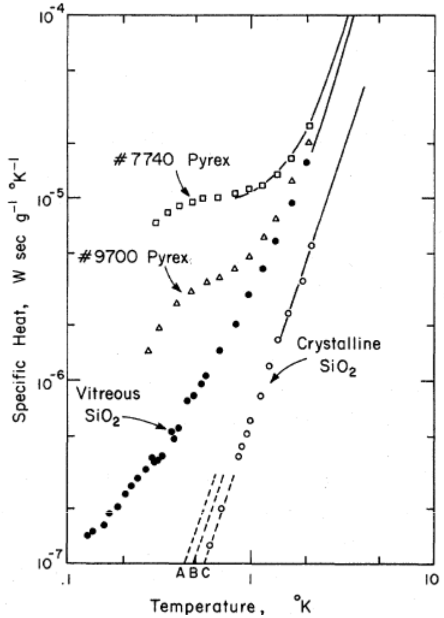

Low Thermal Conductivity:

$$du / dSdt$$

$$= -\lambda . dT / dx$$

(mean free path)

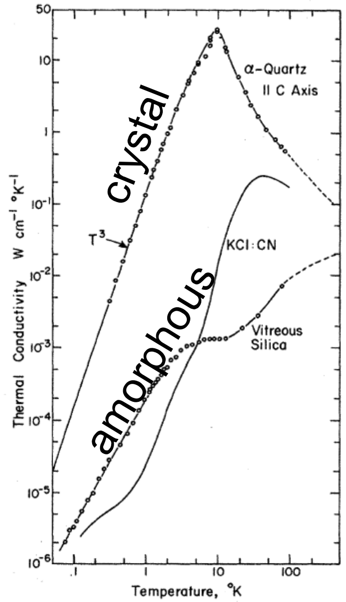

Macroscopic and **Microscopic** description of the **Elastic Behaviour**:

Classical Theory of Elasticity:

$$\delta E = \underline{\underline{\sigma}}^0 : \underline{\underline{\varepsilon}} + \frac{1}{2}\underline{\underline{\varepsilon}} : \underline{\underline{\underline{\underline{C}}}} : \underline{\underline{\varepsilon}} + \ldots.$$

linearized strain tensor $\varepsilon_{\alpha\beta} \equiv \frac{1}{2}\left(\frac{\partial u_\alpha}{\partial x_\beta} + \frac{\partial u_\beta}{\partial x_\alpha}\right)$

stress tensor $\boxed{\sigma_{ij} \equiv \frac{\partial E}{\partial \varepsilon_{ij}} \approx \sigma_{ij}^0 + \sum_{k,l} C_{ijkl} \cdot \varepsilon_{kl}}$

Hoole's Law: 21 Elastic Moduli $C_{\alpha\beta\gamma\delta}$
in the most general 3D case.
2 Elastic Moduli in the isotropic case:

$$\sigma_{\alpha\beta} = \sigma_{\alpha\beta}{}^0 + \lambda . tr \underline{\underline{\varepsilon}} . \delta_{\alpha\beta} + 2\mu . \varepsilon_{\alpha\beta}$$

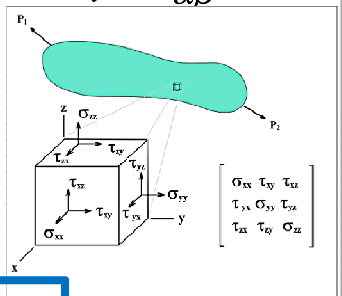

Equations of motion:

$$\rho \frac{\partial^2 \underline{u}}{\partial t^2}(\underline{r}) = \nabla . \underline{\underline{\sigma}} + \underline{f}$$

$$\boxed{\rho \frac{\partial^2 \underline{u}}{\partial t^2}(\underline{r}) = \nabla . (\underline{\underline{\underline{\underline{C}}}}(x,y,z) : \underline{\underline{\varepsilon}}) + \underline{f}}$$

Atomic Scale Description:

$$E(\{\underline{r}_{ij}\}) = \sum_{(i,j)} E_{ij}(\underline{r}_{ij}) + \sum_{(i,j,k)} E_{ijk}(\underline{r}_{ij}, \underline{r}_{jk}, \underline{r}_{ik}) + \ldots$$

2-body interactions
(Cauchy model)
Ex. Lennard-Jones
Foams
BKS model for Silica

3-body inter.
Ex. Silicon

Displacements $\underline{u}(\underline{r}_i) \equiv \underline{r}_i - \underline{r}_i{}^0$

Equations of motion on the particles:

$$\boxed{m_i . \frac{\partial^2 u_\alpha}{\partial t^2}(\underline{r}_i) = -\frac{\partial E_{total}}{\partial r_{i\alpha}} \approx -\sum_j M_{ij}^{\alpha\beta} . u_\beta(\underline{r}_j) + f_\alpha(\underline{r}_i)}$$

Molecular Dynamics Simulations:

$$\boxed{m_i \frac{d\vec{v}_i}{dt} = \vec{F}_i}$$

E=cste in the *Micromechanical* ensemble (isolated system. No damping):

$$\vec{F}_i = -\frac{\partial}{\partial \vec{r}_i} \left(\mathcal{V}(\vec{r}_1, \vec{r}_2, ..., \vec{r}_N) \right)$$

$$E = \mathcal{H}(\vec{r}_i, \vec{p}_i) = \sum_i \frac{p_i^2}{2m_i} + \mathcal{V}(\vec{r}_1, \vec{r}_2, ..., \vec{r}_N)$$ Total energy

T=cste in the *Canonical* ensemble:

$$< E_c >= \frac{3}{2} N k_B T \qquad \sum_i \mathrm{m_i} \delta \mathrm{v_i^2} = \mathrm{cste}$$

Different choices of Thermostats:

Langevin: $m_i \frac{dv_i}{dt} = -\Gamma . v_i + F_i + \kappa(t)$ with $<\kappa(t).\kappa(t')>=\mathrm{cste}.2\Gamma k_B T.\delta(t-t')$

Andersen: *prob. of collision $\nu\Delta t$. Maxwell-Boltzman velocity distr.*

Nosé-Hoover:

$$\boxed{\begin{aligned} m_i \frac{d\vec{v}_i}{dt} &= \vec{F}_i - m_i \zeta \vec{v}_i \\ Q \frac{d\zeta}{dt} &= \sum_i m_i \vec{v}_i^2 - (3N+1) k_B T \end{aligned}}$$

Simple Rescaling: $(\delta \mathrm{v_{new}} / \delta \mathrm{v_{old}})^2 = \mathrm{T} / \mathrm{T_{inst}}$

Berendsen: $v_i' = \lambda v_i$ with $\lambda = \left(1 - \frac{dt}{\tau}\left[\frac{T}{T_0} - 1\right]\right)^{1/2}$

Microscopic determination of **different physical quantities**:

-**Density** profile, pair distribution function $\hat{\rho}(\vec{r}) = \sum \delta(\vec{r} - \vec{r}_i)$

$$\rho^{(2)}(\vec{r}, \vec{r}') = < \hat{\rho}(\vec{r})\hat{\rho}(\vec{r}') > \equiv \lim_{\tau \to \infty} \frac{1}{\tau} \int_0^{\tau} \hat{\rho}(\vec{r}, t)\hat{\rho}(\vec{r}', t)dt \qquad g(\vec{r}, \vec{r}') = \rho^{(2)}(\vec{r}, \vec{r}')/\rho(\vec{r})\rho(\vec{r}')$$

$$S(\vec{k}) = \frac{1}{N} < \sum_{i,j} \exp\left(-i\vec{k}.(\vec{r}_j - \vec{r}_i)\right) >$$

-**Velocity** profile

-**Diffusion constant** $D = \frac{1}{6t} < (\vec{r}_i(t) - \vec{r}_i(0))^2 > = \frac{1}{3} \int_0^{\infty} < \vec{v}_i(t).\vec{v}_i(0) > dt$

-**Stress tensor** (Irwin-Kirkwood, Goldenberg-Goldhirsch)

$$P_{\alpha\beta} = \sum_i \frac{p_{i\alpha} p_{i\beta}}{m_i} + \sum_i r_{i\alpha} F_{i\beta}$$

-**Pressure** $PV = Nk_B T + \frac{1}{3} < \sum_i \vec{r}_i.\vec{F}_i > \longrightarrow$ $\boxed{\textbf{Barostat}}$

-**Strain** $u_{ij}^{P} = \underline{u}_{ij} . \frac{\underline{r}_{ij}^{eq}}{r_{ij}^{eq}} \approx \sum_{\alpha} \sum_{\beta} \frac{r_{ij}^{eq,\alpha} . r_{ij}^{eq,\beta}}{r_{ij}^{eq}} . \varepsilon_{\alpha\beta}$

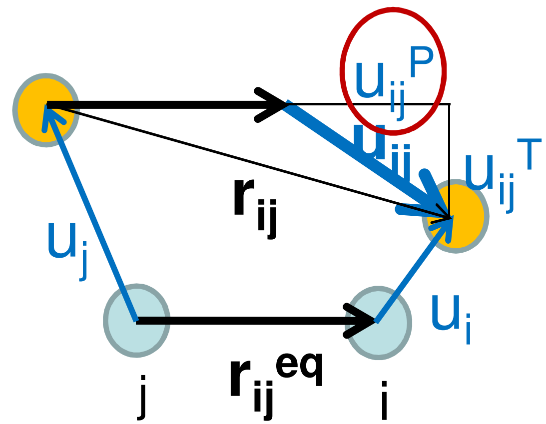

Length Scales:

Elastic Moduli:

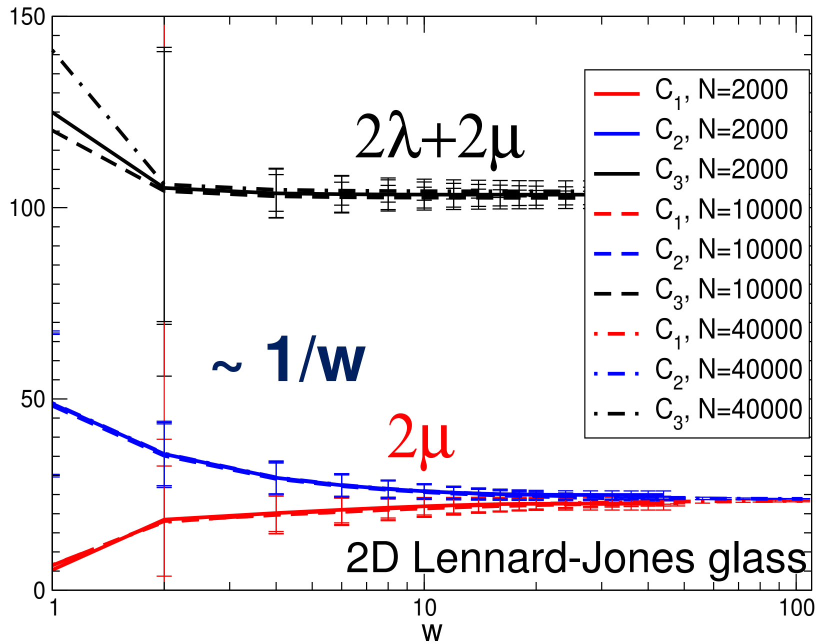

Coarse Graining ← Linear Elasticity

W	0	5	10	15	20 a
Hooke's law	NO	YES	YES	YES	YES
Homogeneity $\frac{<\epsilon>(W)-2\mu}{2\mu}<10\%$	NO	NO	YES	YES	YES
$\frac{\Delta C}{<c>}<10\%$	NO	NO	NO	YES	YES
Isotropy $\frac{C_2-C_1}{2\mu}<10\%$	NO	NO	NO	NO	YES

M. Tsamados et al. EPJE (2009)

Isotropic Elasticity

Eigenfrequencies:

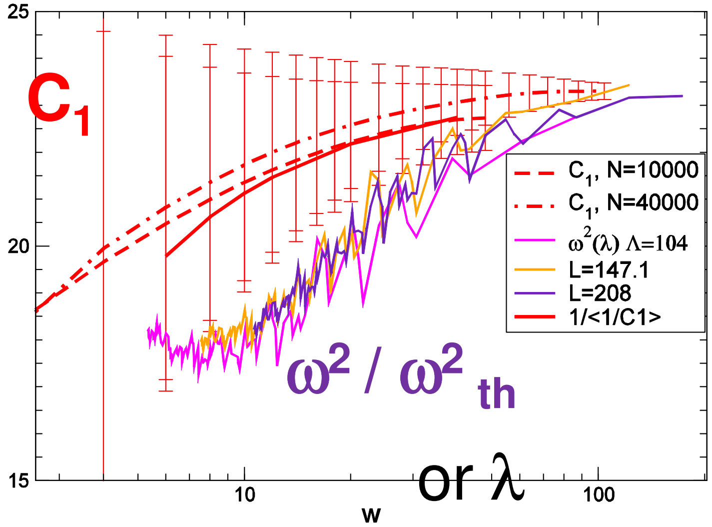

$\omega^2{}_{th} \sim C_{1\infty}/\lambda$

$\omega \longrightarrow \omega_{th}$ for $\lambda > 20a \sim 2$ nm

Box Size L> 2 nm

A. Tanguy et al. PRE (2002)

2D Lennard-Jones Glass:

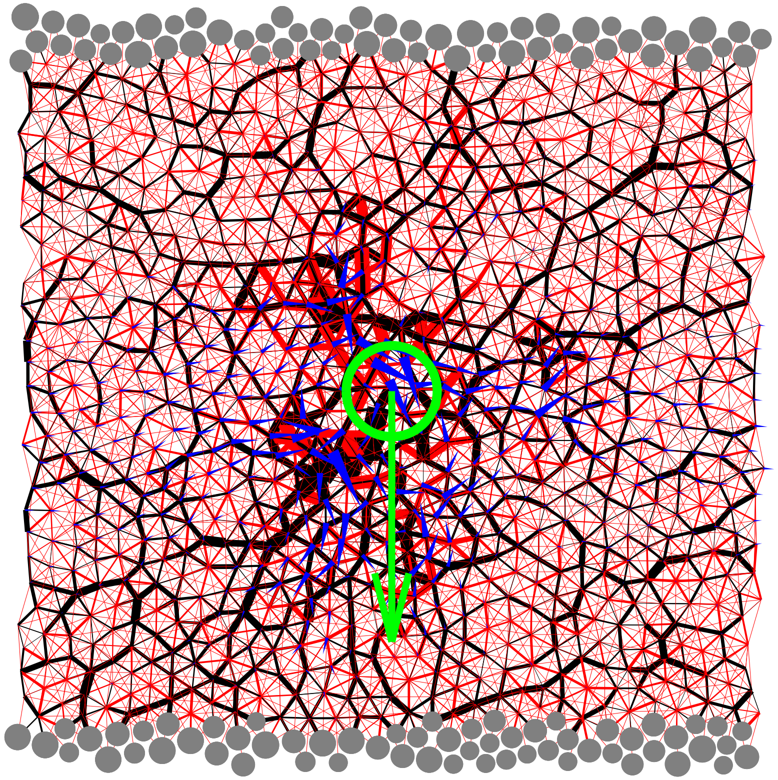

F. Léonforte et al (2004)

Heterogeneous Displacements

Large fluctuations

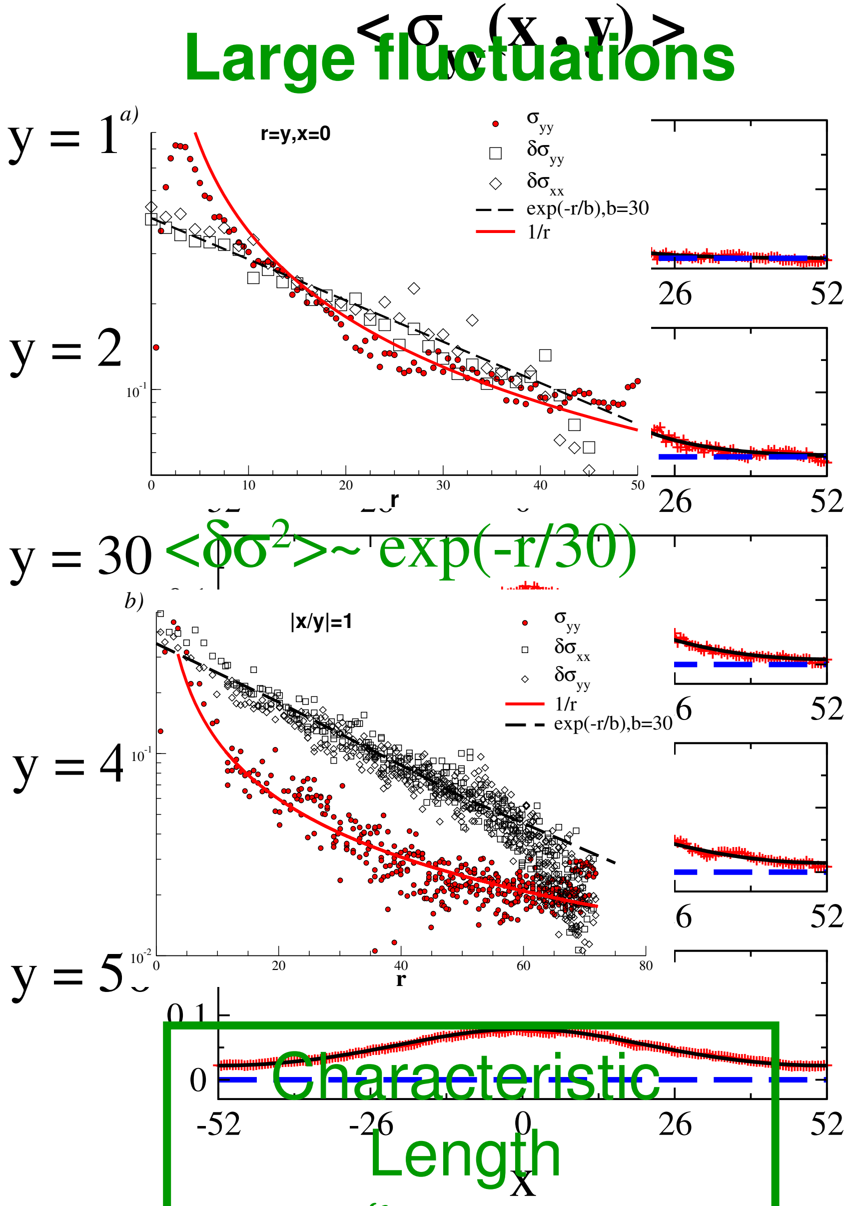

$<\delta\sigma^2>\sim \exp(-r/30)$

Characteristic Length
$\xi \sim 30\ \sigma$

Time Scales:

Length scales $a_{ij} \approx 10$ Å
Masses $m_i \approx 10^{-25}$ kg
Energy $\varepsilon_{ij} \approx 1$ eV $\approx 2.10^{-19}$J $\approx k_B T_m$

Time scale $\tau \approx \sqrt{\dfrac{m_i . a^2}{\varepsilon_{ij}}} \approx 10^{-12}\,\mathrm{s}$ or $\tau \approx \dfrac{(0.1a)^2}{D(T=1)} \approx \dfrac{10^{-20}}{10^{-8}} \approx 10^{-12}\,\mathrm{s}$

$N=10^6$ particles, Box size $L=100\sigma \approx 10$ nm for a mass density $\rho=1$.
$3.N.N_{neig} \approx 10^8$ operations at each « time » step.

Time step $\Delta t = 0.01\tau \approx 10^{-14}$ s
10^6 MD steps $\approx 10^{-8}$ s = 10 ns or $10^6 \times 10^{-4}$=100% shear strain in quasi-static simulations

Quench rate ~ 1000 °K/ 10 ns = 10^{11} °K/s >> 10^6 °K/s

Thermal Regimes:

Athermal Limit

M. Tsamados et al. (2010)

Typical Relative displacement due to the **external strain** $a.\dot{\gamma}.t$

larger than $\vee\vee$

Typical vibration of the atom due to **thermal activation** $\sqrt{\frac{k_B T}{k_h}}$

$$\boxed{\sqrt{\frac{k_{\rm B}{\rm T}_c}{m\omega_0^2}} \lesssim \frac{2\pi\dot{\gamma}\sigma}{\omega_0},}$$

Ex. Lennard-Jones systems:

$\mathrm{T}_c \lesssim 40\dot{\gamma}^2$ $\quad$ $\mathrm{T}_c \approx 4.10^{-3}$ at $\dot{\gamma} = 10^{-2}$

$\omega_0 = \sqrt{k_h/m}$ $\quad$ $\mathrm{T}_c \approx 4.10^{-7}$ at $\dot{\gamma} = 10^{-4}$

Ex. Colloids: $\quad$ $\mathrm{T} = 300°\mathrm{K}$ $\quad$ $\dot{\gamma} > 10^{-6}\mathrm{s}^{-1}$

Efficient Damping

F. Varnik et al. (2008)

Time needed to **dissipate** heat created $\quad$ $t_d = \frac{L}{c}$

smaller than $\wedge\wedge$

Time needed to generate $\mathbf{k_B T}$ by **plastic activation** $\quad$ $t_Q = \frac{k_B T}{\sigma_{xy}.\dot{\gamma}}$

$$\boxed{\dot{\gamma} << \frac{k_B T.c}{L.\sigma_{xy}\left(\dot{\gamma}\right)}}$$

after setting $T=0.2$ and $\sigma \approx 0.6$, yields

$\dot{\gamma}_{\rm tot} \lesssim 3\times10^{-2}$.

Athermal Regime: **2D Lennard Jones T=10^{-7}**

at constant Strain Rate and Temperature

M. Tsamados (2010)

Competition between nucleation and diffusion

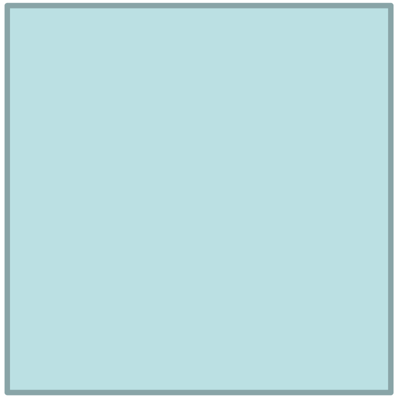

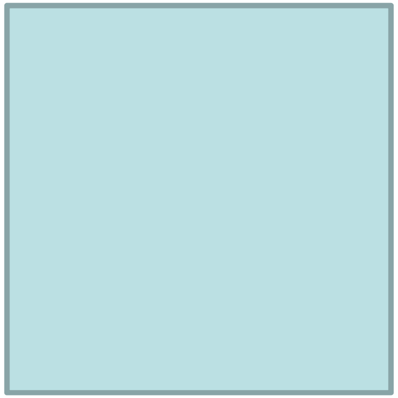

Low strain rate $\dot{\gamma} = 10^{-4}$

Progressive Diffusion of Local Rearrangements

Finite Size Effects

Large strain rate $\dot{\gamma} = 10^{-3}$

Nucleation of Local Rearrangements

Non-Uniform Temperature Profile and viscosity
Efficient damping regime - F. Varnik (2008)

Visco-Plastic Behaviour:

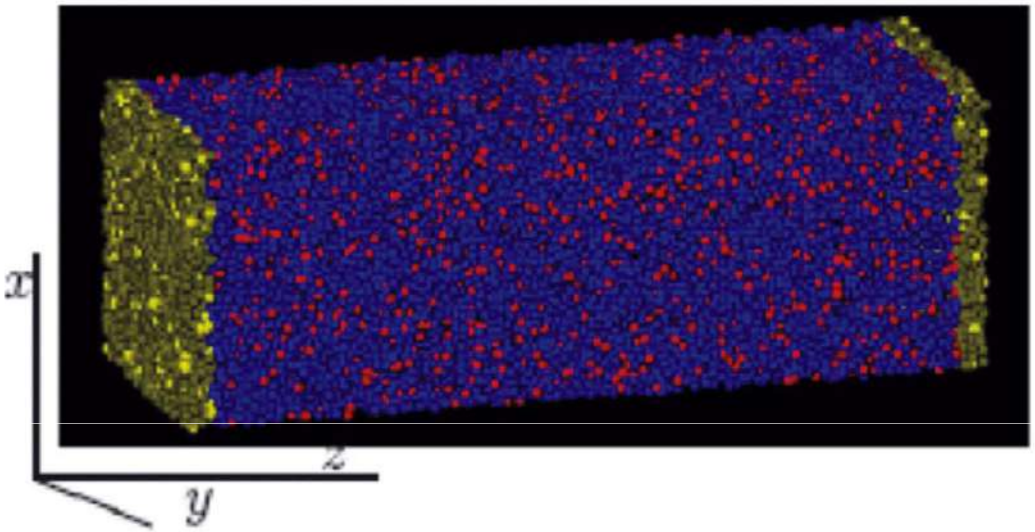

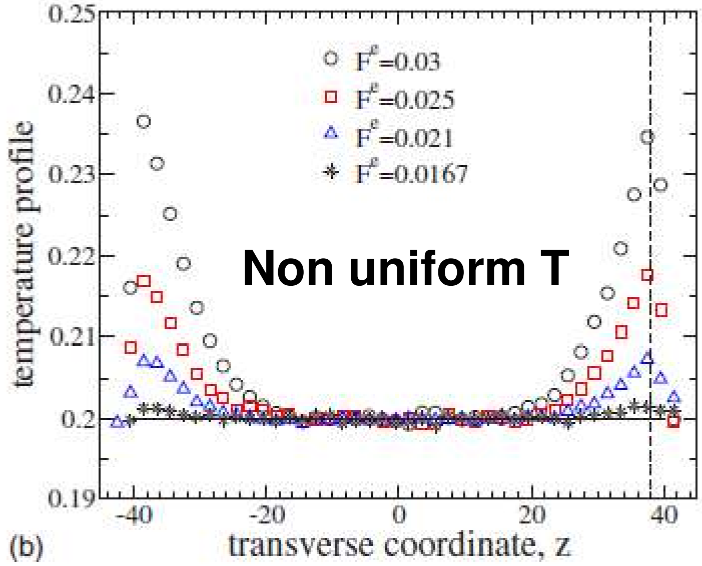

Non uniform T

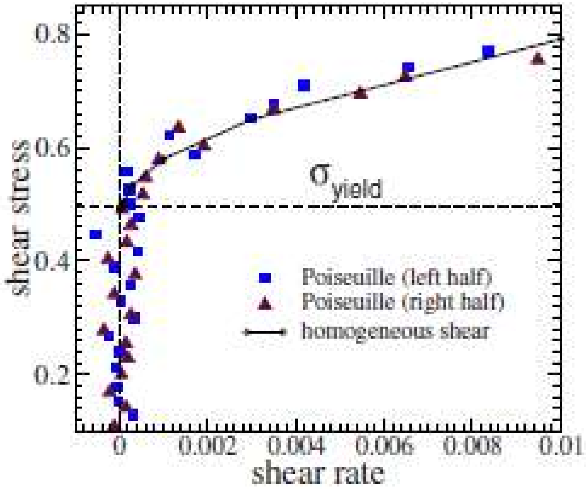

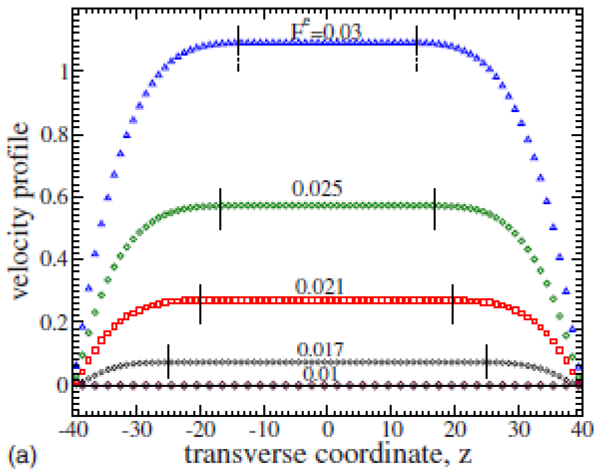

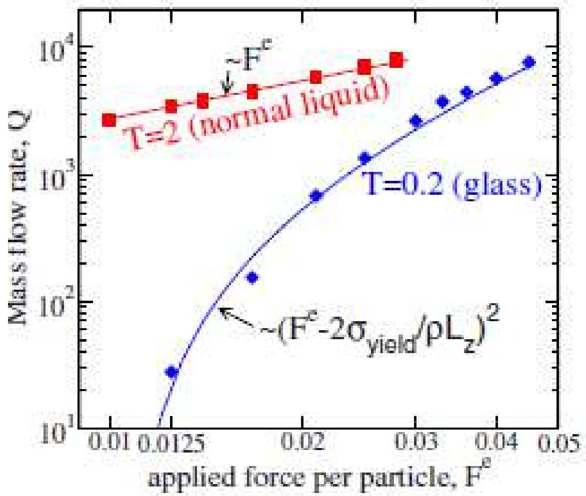

Energy Minimization

quasi-static simulations in the athermal limit:

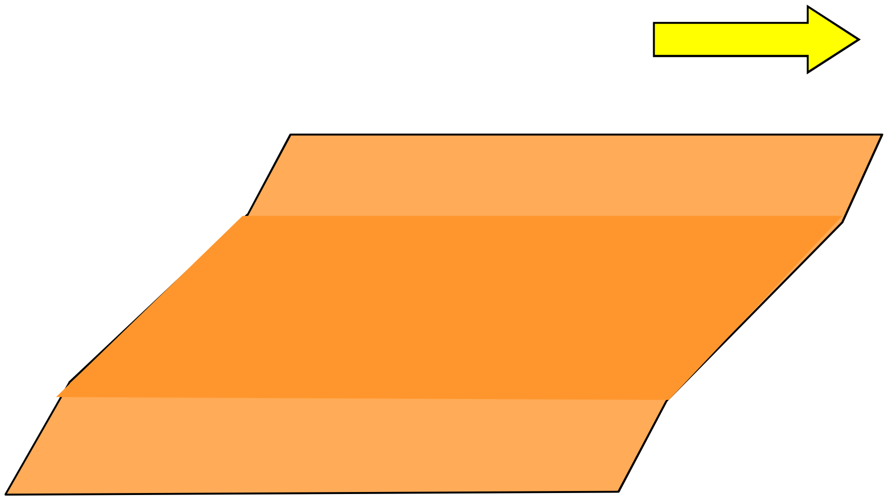

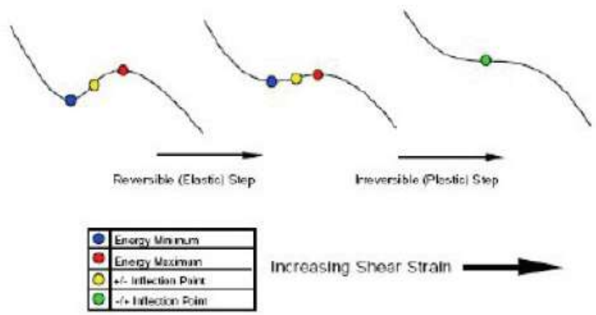

At each step, apply a small strain δε (L) ≈ 10^{-4} on the boundary,
and Relax the system to a local minimum of the Total Potential Energy V({ri}).
Dissipation is assumed to be total during δε.

Quasi-Static Limit

$$\delta t >> a / c \approx 10^{-12}\,\mathrm{s}$$

$$\frac{\delta\varepsilon}{\delta t} << \frac{\delta\varepsilon.\mathrm{c}}{\mathrm{a}} << \frac{\varepsilon_{\lim}(\mathrm{L}).\mathrm{c}}{\mathrm{a}} \approx 10^{7}\,\mathrm{s}^{-1}(\approx 10^{-5}\,\mathrm{u}_{\mathrm{LJ}}).$$

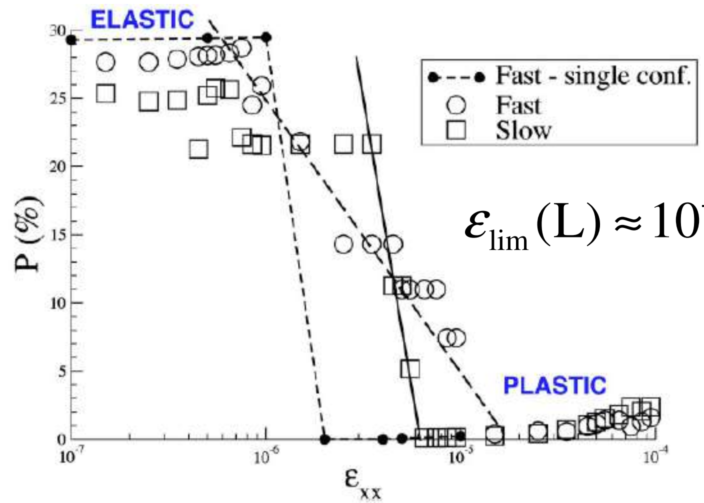

$$\varepsilon_{\lim}(\mathrm{L}) \approx 10^{-5}$$

MD versus Energy MInimization in the athermal limit:

At $T=10^{-8}$ (rescaling of the transverse velocity v_y et each step)

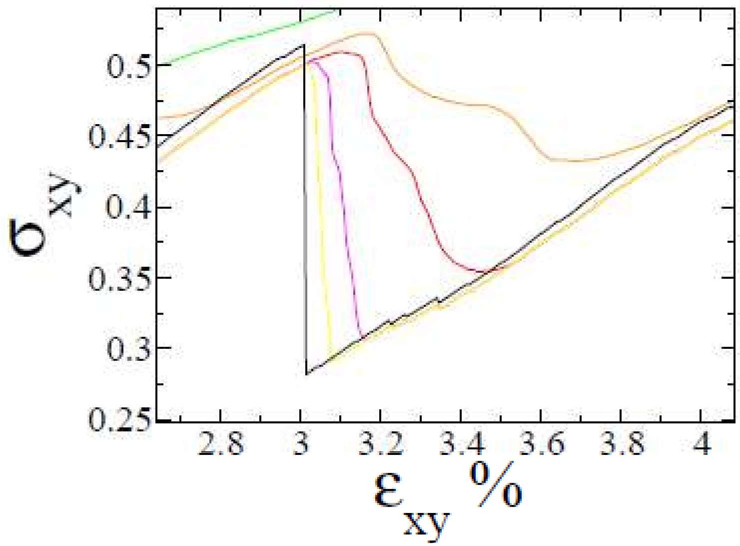

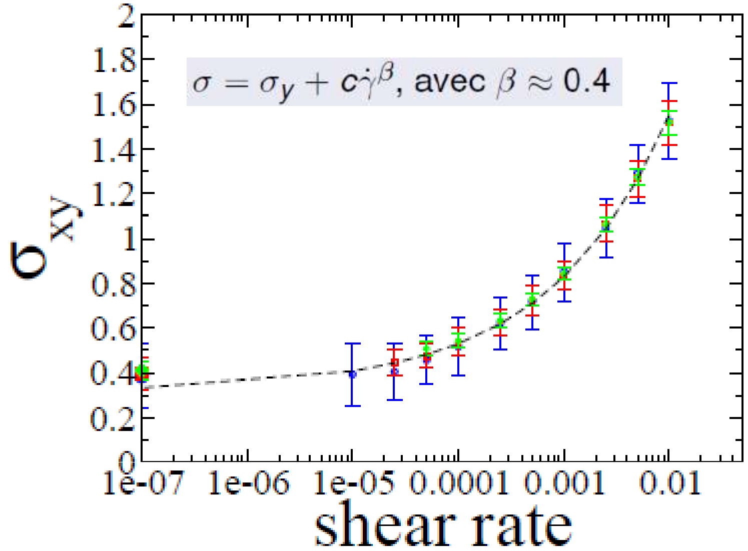

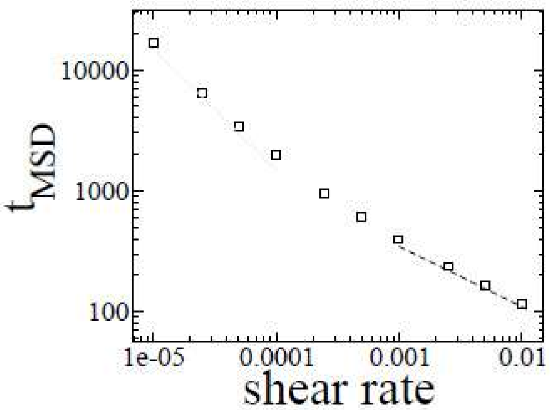

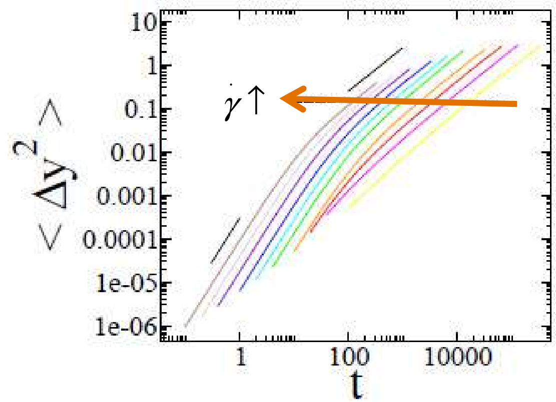

M. Tsamados (2010)

$\dot{\gamma} \gtrsim \dot{\gamma}_c \Rightarrow t_{1/e} \propto \dot{\gamma}^{-\nu_2}$, $\nu_2 \approx 0.6$ (régime dynamique)

$\dot{\gamma} \lesssim \dot{\gamma}_c \Rightarrow t_{1/e} \propto \dot{\gamma}^{-1}$ (régime QS)

$$\sigma \approx \eta.\dot{\gamma} \approx \left(\dot{\gamma}\right)^{0.4}$$

$$\sigma \approx \eta.\dot{\gamma} \approx cste$$

The Stress-Strain behaviour in the QS limit:

A. Tanguy et coll. Phys. Rev. B (2002), J.P. Wittmer et coll. Europhys. Lett. (2002), A. Tanguy et coll. App. Surf. Sc. (2004)
F. Léonforte et coll. Phys. Rev. B (2004), F. Léonforte et coll. Phys. Rev. B (2005), F. Léonforte et coll. Phys. Rev. Lett. (2006),
A. Tanguy et coll. (2006), C. Goldenberg et coll. (2007), M. Tsamados et coll. (2008), M. Talati et coll. (2009).

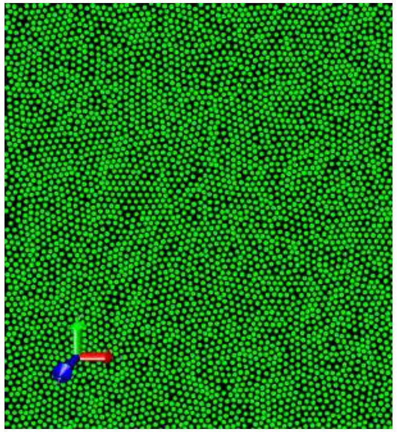

Atomic displacements:

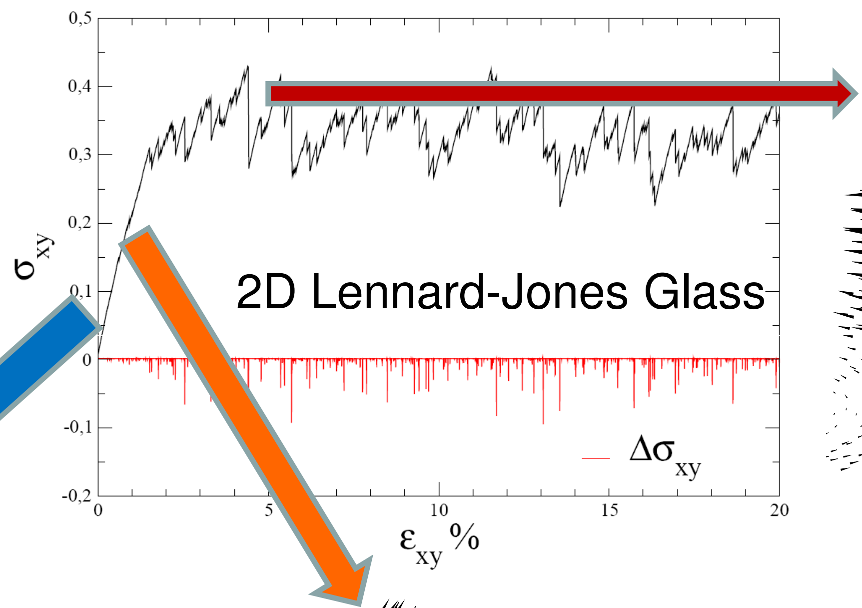

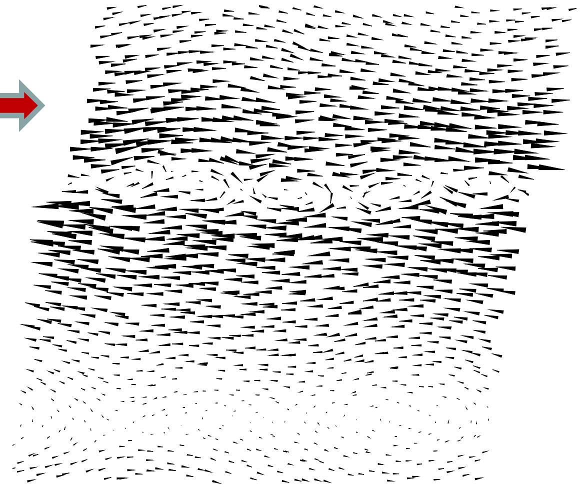

Elementary Shear band (x0.4)

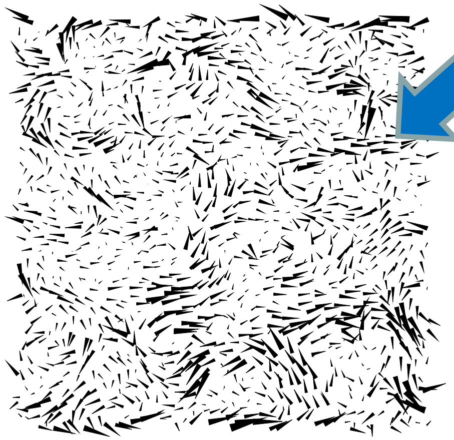

Non-affine **reversible** displacements ($\times 10^3$)

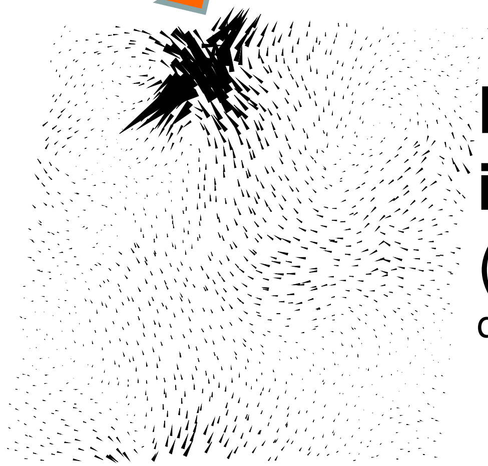

Local shear **ir**reversible (x40)
quadrupolar event

Silica-like glass

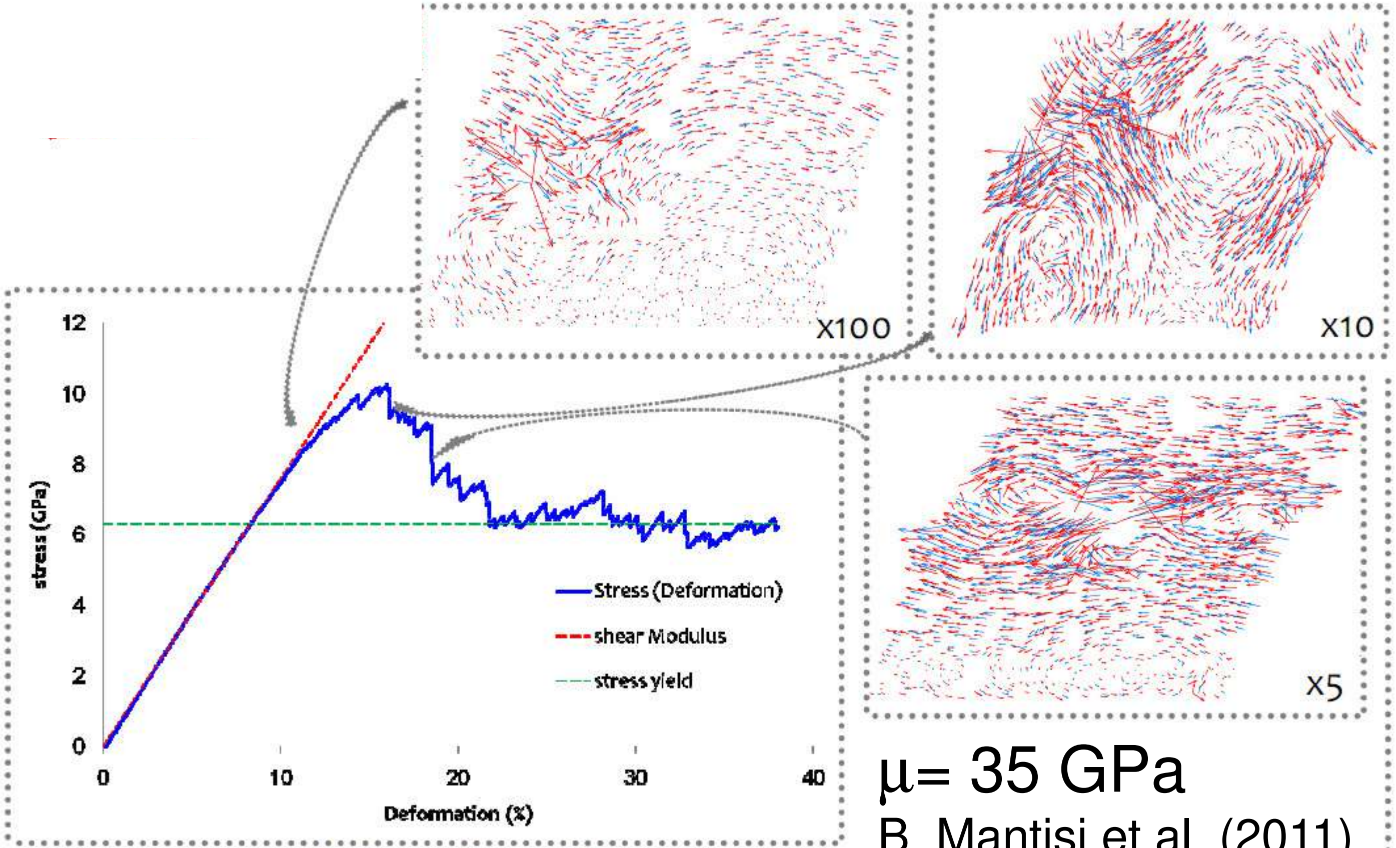

Figure 2.a – Hook's Law from 0 to 40 % of BKS silica.

μ= 35 GPa

B. Mantisi et al. (2011)

BKS Potential. P_0=0 Gpa. N=24 000 atoms. L=71.66 Å

$$\phi_{\alpha\beta}^{BKS}(r) = \frac{E_{\alpha\beta}}{r} + \left(A_{\alpha\beta} e^{-B_{\alpha\beta} \cdot r} - \frac{C_{\alpha\beta}}{r^6} \right) + \left(\frac{D_{\alpha\beta}}{r} \right)^{12}$$

A. Carré et al. (2007)

a-Silicon

$$E_{SW}(1,2,\ldots,N)=\Sigma_{(i,j)}(A.r_{ij}^{-4}-B).e^{(r_{ij}-a)^{-1}}+\Sigma_{i,j,k}\lambda.\left(\cos\theta_{jik}+\frac{1}{3}\right).e^{\gamma.(r_{ij}-a)^{-1}+\gamma.(r_{ik}-a)^{-1}}$$

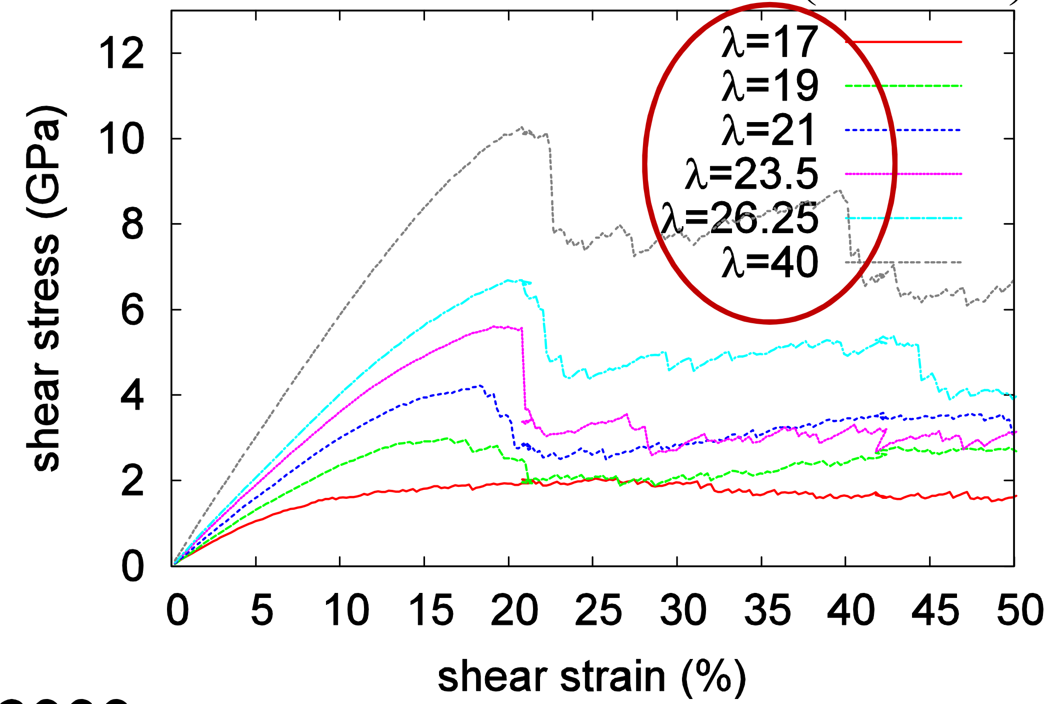

C. Fusco et al. (2010)

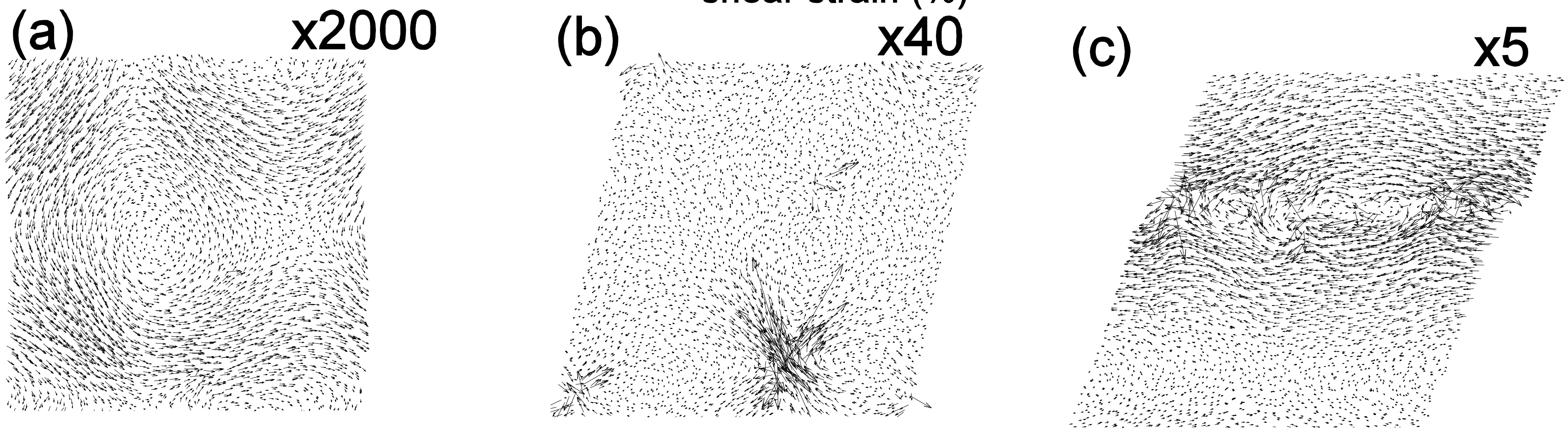

Effect of
the **three body interaction** λ:

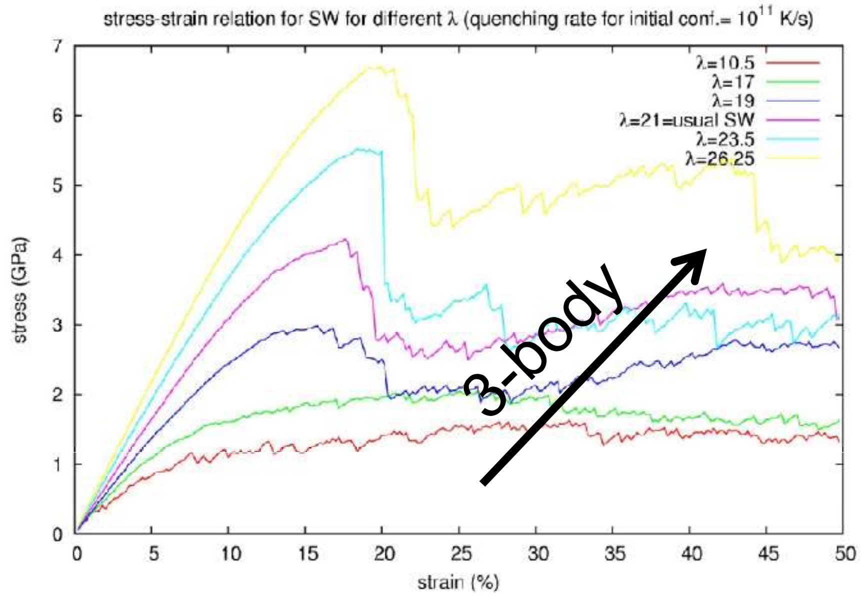

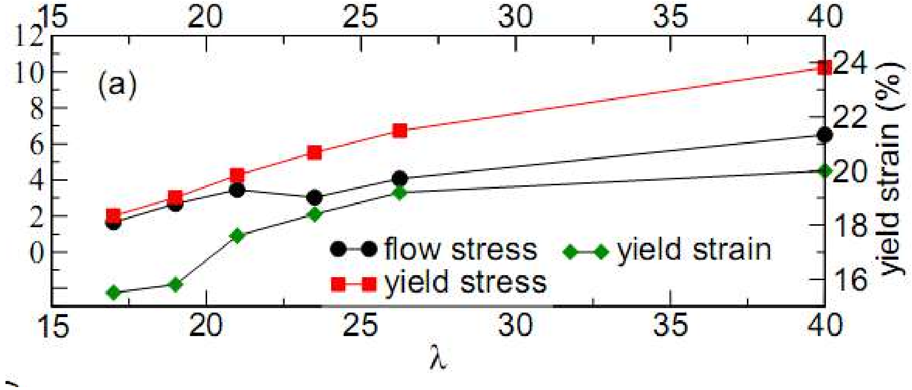

Effect of
the **quenching rate** (structure):

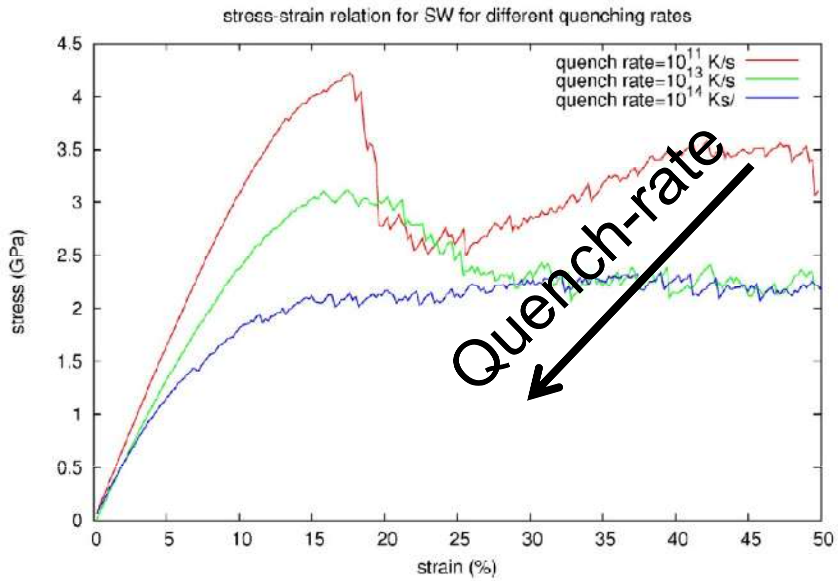

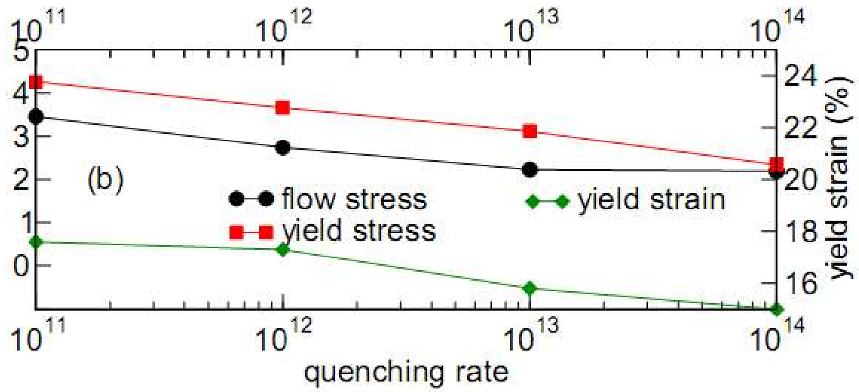

Transition to **strain softening**, and **heterogeneous** flow.

Quasi-Static Response of Silica Glass under Hydrostatic Pressure

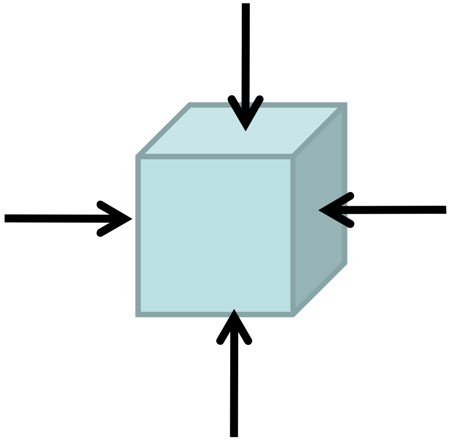

Load ≠ Unloading

Irreversible densification from P ≈ 13 GPa

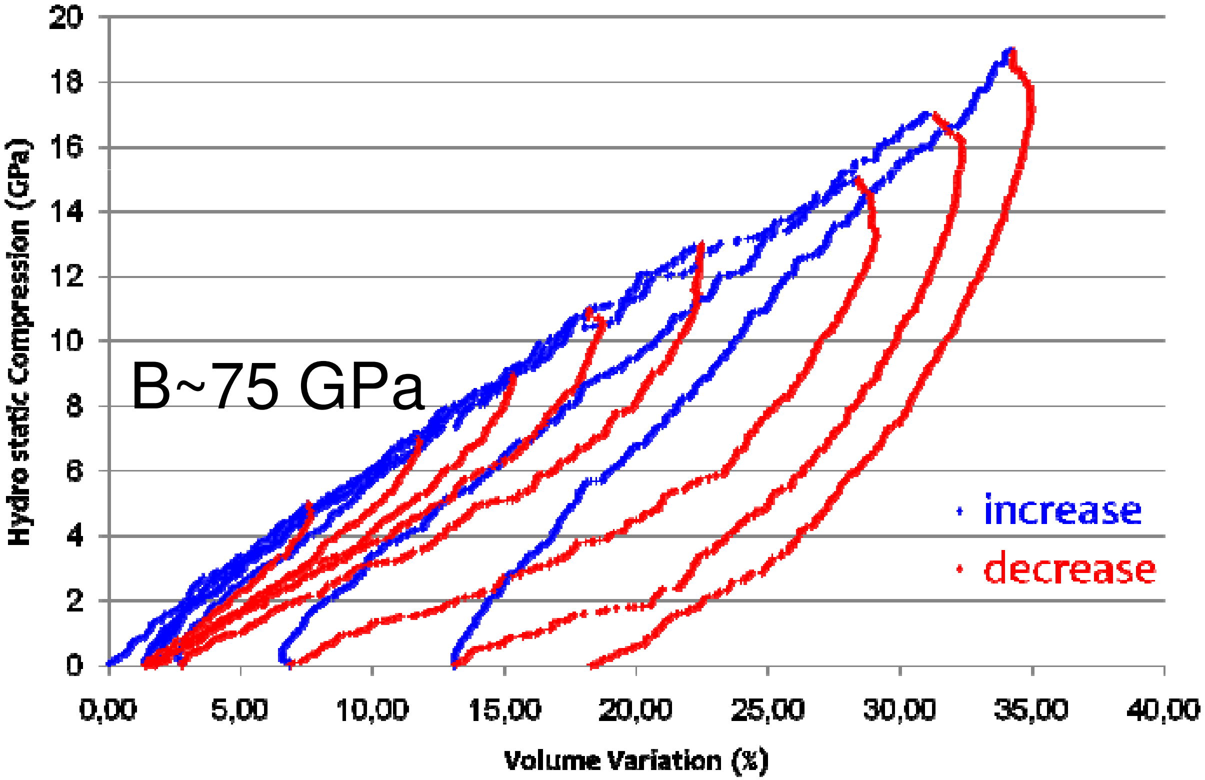

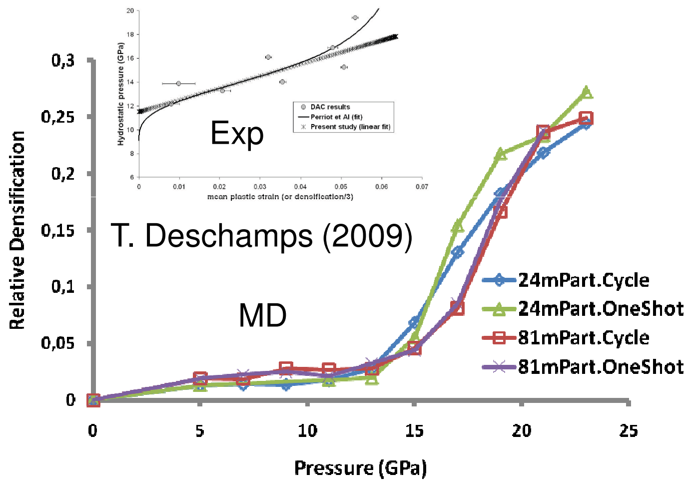

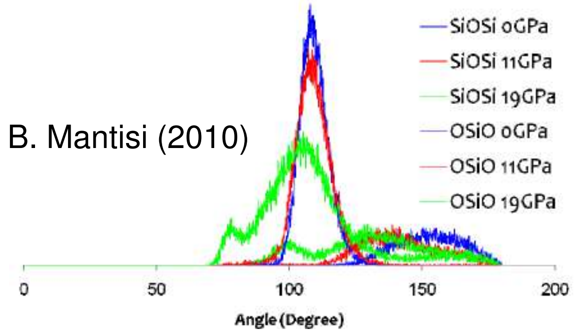

Mesoscopic Modelling:

Local rules and Long-range elastic Couplings

Ex. Roux et al. (2000)
Picard et al. (2002)
Dahmen et al. (2005)

Local Plastic Threshold
+
Long-range Elastic interactions

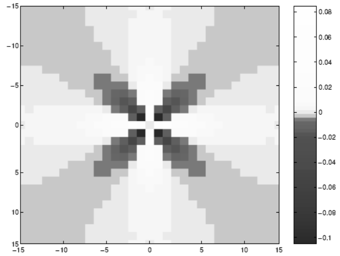

$$\epsilon_p(x,t) = \sum_{1}^{t} \eta(t)\delta(x - x^*(t))$$

$$\sigma^1_{xy}(\mathbf{r}) = 2\mu \int d\mathbf{r}' G^\infty(\mathbf{r}-\mathbf{r}')\epsilon^{\mathrm{pl}}_{xy}(\mathbf{r}')$$

$$G^\infty(r,\theta) = \frac{1}{\pi r^2}\cos(4\theta)$$

D. Vandembroucq et al. (2011)

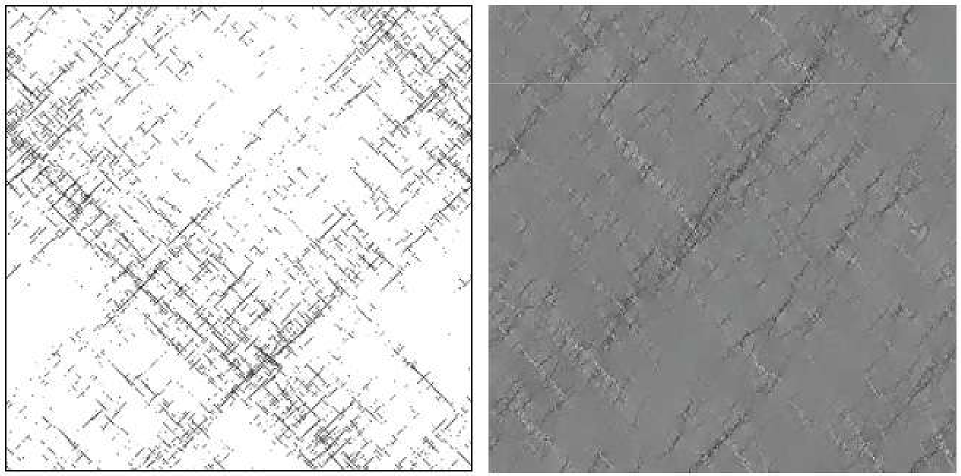

Figure 1. Left: Map of cumulated plastic activity in the stationary regime during a deformation window $\Delta\varepsilon = 0.01$ obtained with a mesoscopic model of amorphous plasticity[31]. A "diffuse" localization of the plastic deformation is observed along axes at $\pm\pi/4$. Right: for comparison, reproduction of a strikingly similar map of plastic activity (vorticity of the displacement field)[17]) on a 2D Lennard-Jones glass under compression.

II. Statistical Analysis

local dynamics

correlated motion

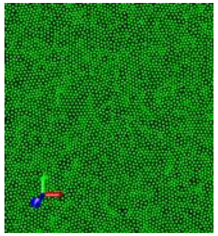

Local Dynamics: Motion of an individual particle

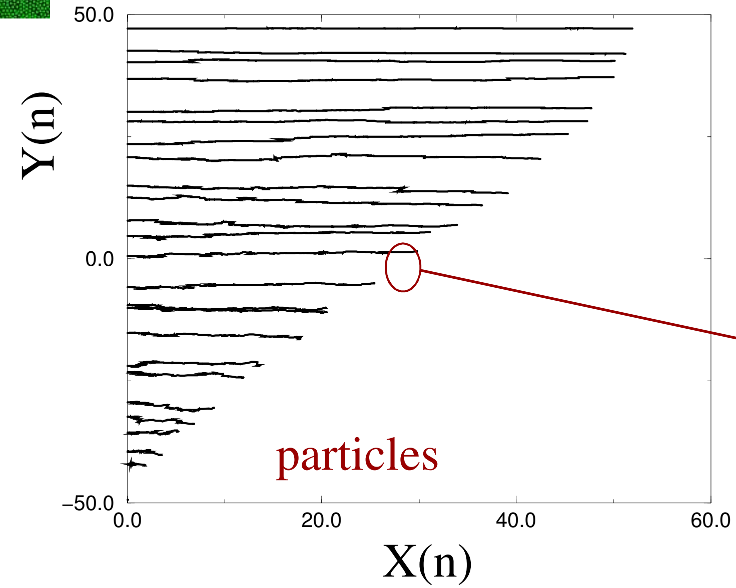

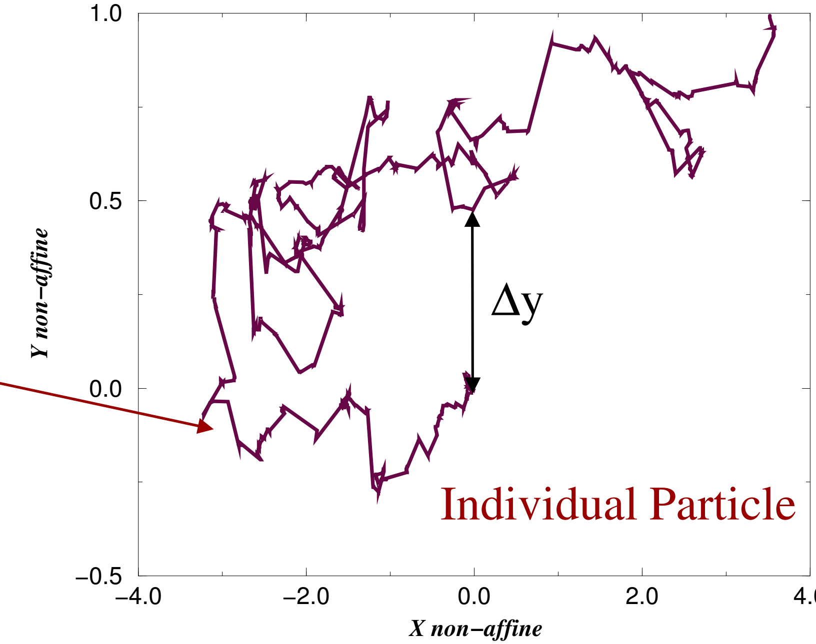

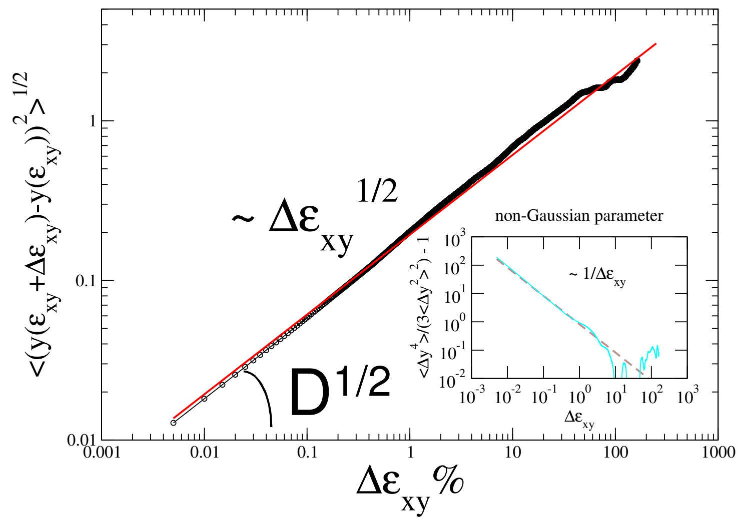

Non-Gaussian Motion.

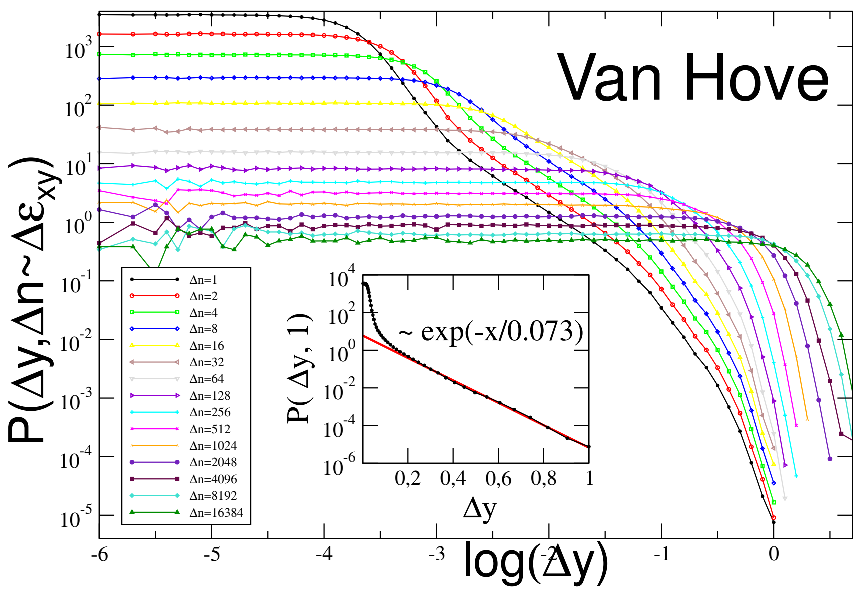

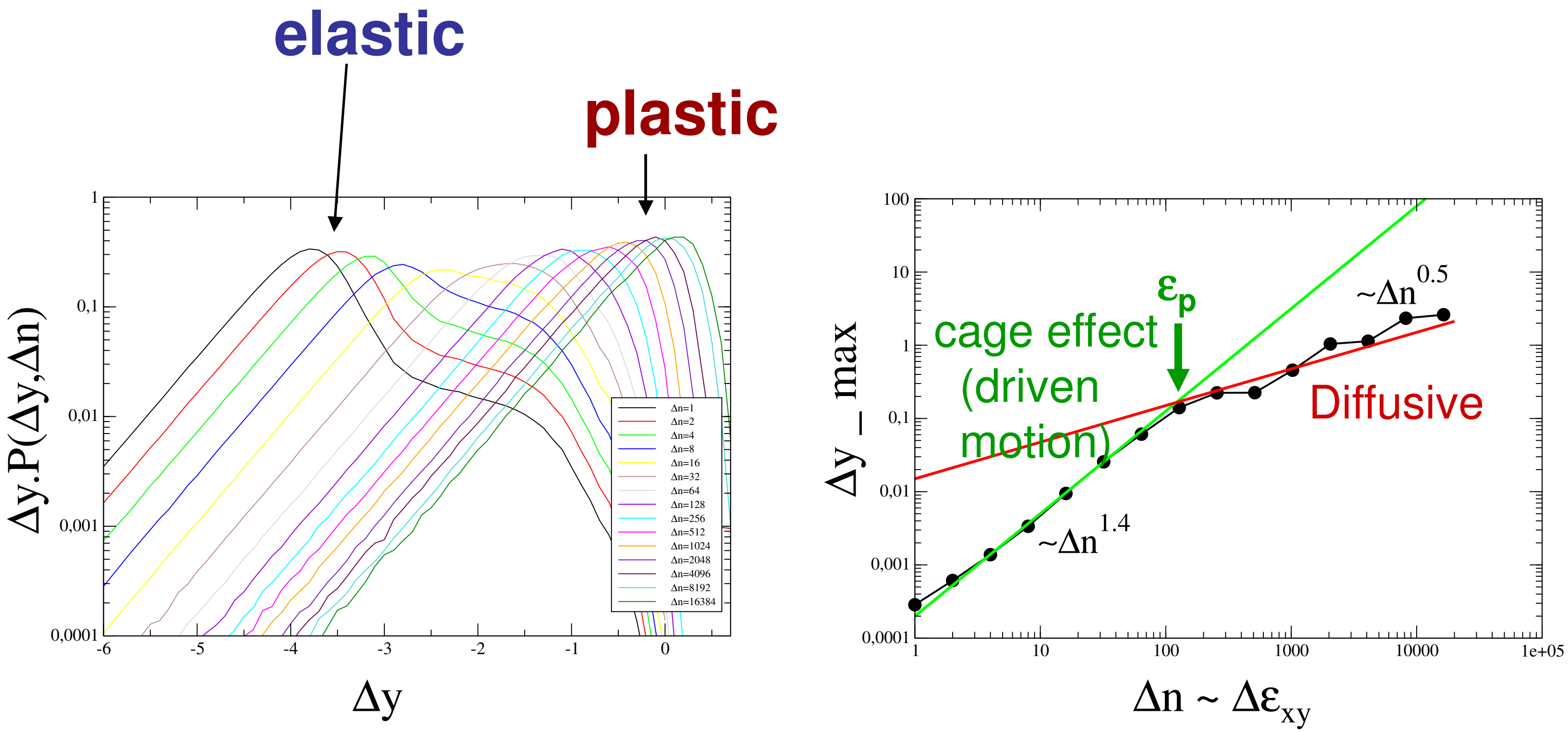

External Driving allows to recover a Diffusive Motion.

Tanguy et al. (2006), Besseling, Weeks et al. (2006), O. Dauchot et al. (2005), Roux et al. (2002)

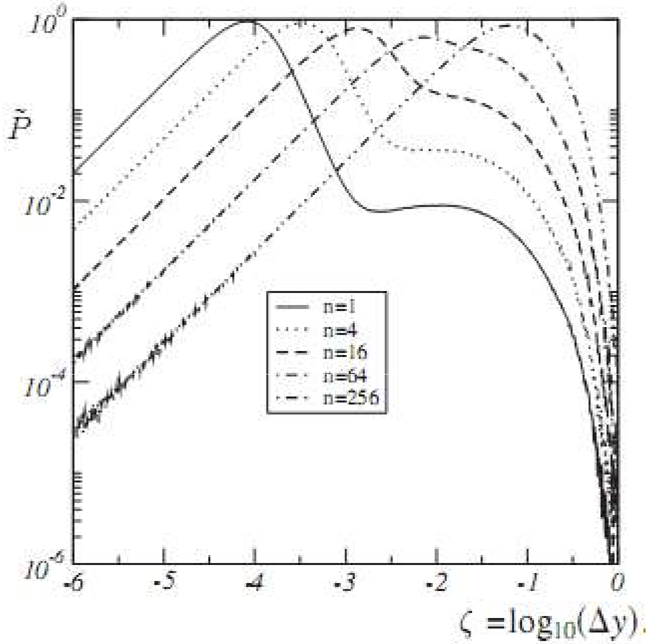

FIG. 3. The distribution $\widetilde{P}(\zeta;\Delta\gamma)$ of the scale variable $\zeta = \log_{10}(\Delta y)$ for increasing values of $n=\Delta\gamma/\delta=1,4,16,64,256$. System size: $L=20$.

A. Lemaitre and C. Caroli (2007)

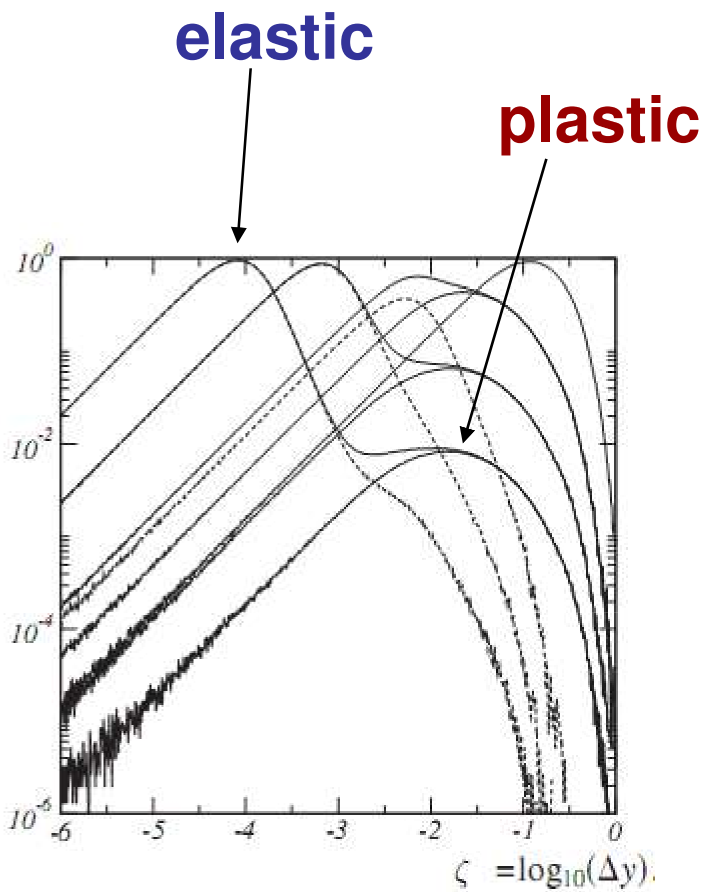

FIG. 4. Decomposition of the total distributions $\widetilde{P}(\zeta;\Delta\gamma)$ (thick solid lines), for $n=\Delta\gamma/\delta=1,8,64,512$. For increasing n's, the maximum of the distribution shifts rightwards. Thin solid lines: contribution of plastic events; thin dashed lines: contribution of elastic branches (see text). System size $L=20$.

Correlated Motion:

Ex. Dynamical Heterogeneities **for T > Tg**:

Direct Experimental Evidence of a Growing Length Scale Accompanying the Glass Transition

L. Berthier,[1*] G. Biroli,[2] J.-P. Bouchaud,[3,4] L. Cipelletti,[1]
D. El Masri,[1] D. L'Hôte,[4] F. Ladieu,[4] M. Pierno[1]

SCIENCE VOL 310 16 DECEMBER 2005

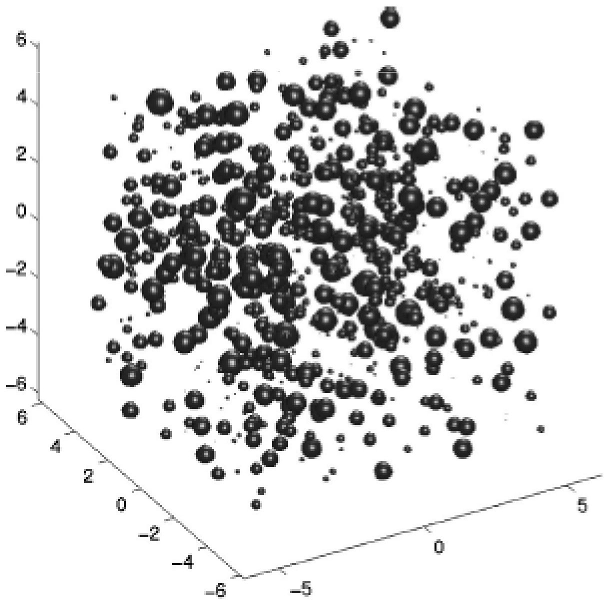

LJ T=2

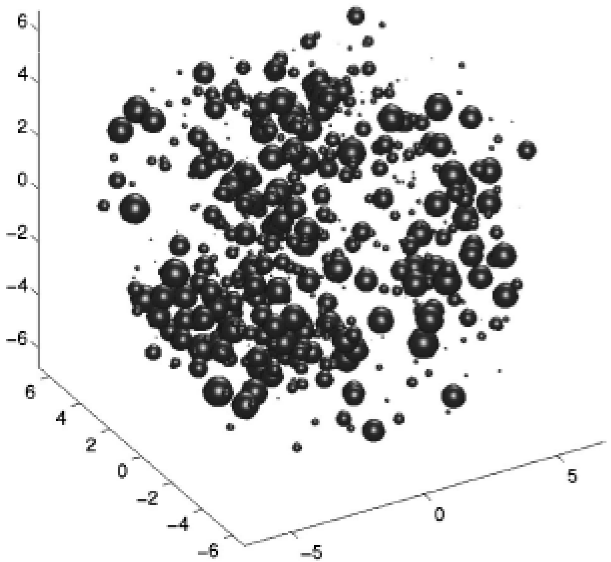

T=0.6

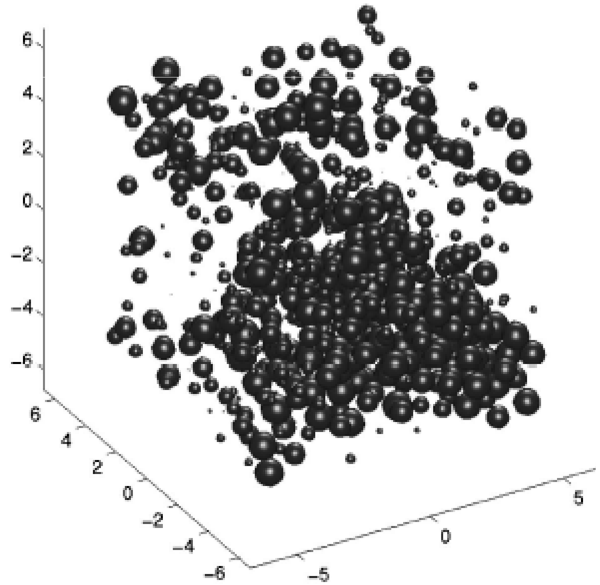

T=0.45 ~ Tg

4-point correlation function χ_4(t) on the local density:

$$\chi_4(t) = \frac{1}{V\rho^2}\int d\vec{r}_1 d\vec{r}_2 \left\langle \rho(\vec{r}_1,0).\rho(\vec{r}_1,t).\rho(\vec{r}_2,0).\rho(\vec{r}_2,t)\right\rangle$$
$$- \left\langle \rho(\vec{r}_1,0).\rho(\vec{r}_1,t)\right\rangle\left\langle \rho(\vec{r}_2,0).\rho(\vec{r}_1,t)\right\rangle$$

$$\chi_4(t) = \frac{1}{V\rho^2}\left[\left\langle Q_p^2(t)\right\rangle - \left\langle Q_p(t)\right\rangle^2\right]$$

$$Q_p(t) = \int d\vec{r}\,\rho(\vec{r},0).\rho(\vec{r},t)$$

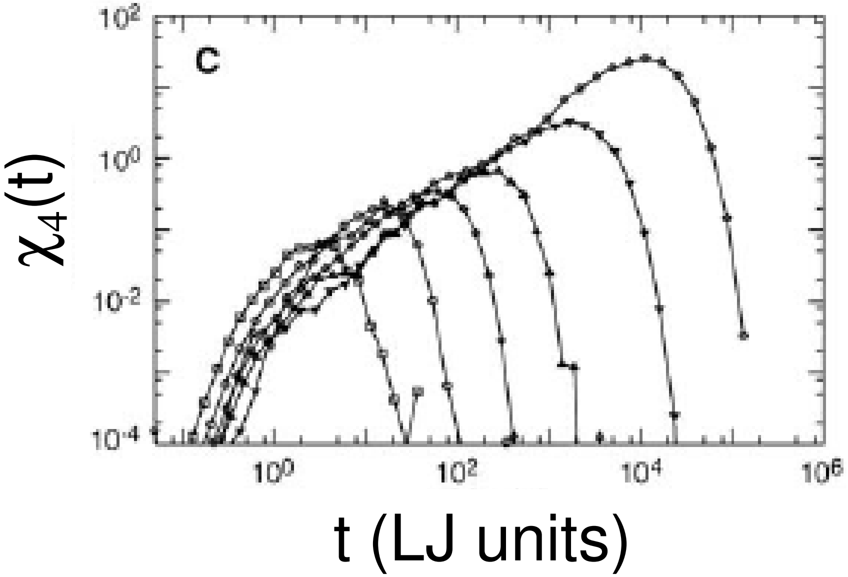

$$N_X^{coop} \equiv \frac{\mathrm{Var}[\Sigma X_i]}{\Sigma \mathrm{Var}[X_i]} = 1 + \frac{\sum_{i\neq j}\langle X_i X_j\rangle}{\Sigma\langle X_i^2\rangle}.$$

$$\chi_4(t) = N_X^{coop}$$
when $X_i \equiv \left(\rho(\vec{r}_i,t) - \langle\rho(t)\rangle\right).\left(\rho(\vec{r}_i,0) - \langle\rho(0)\rangle\right)$

L groups with M identical X_i

$\Rightarrow N_X^{coop} = M$

Binary Lennard-Jones mixture

Dynamical Heterogeneities upon Mechanical load **at T<<Tg**

$$Q_s(a,\epsilon) = \frac{1}{N}\sum_i \exp\left(-\frac{\Delta y_i(\epsilon)^2}{2a^2}\right), \qquad \chi_4(a,\epsilon) = N\left[\langle Q_s(a,\epsilon)^2\rangle_{i,\epsilon} - \langle Q_s(a,\epsilon)\rangle_{i,\epsilon}^2\right]$$

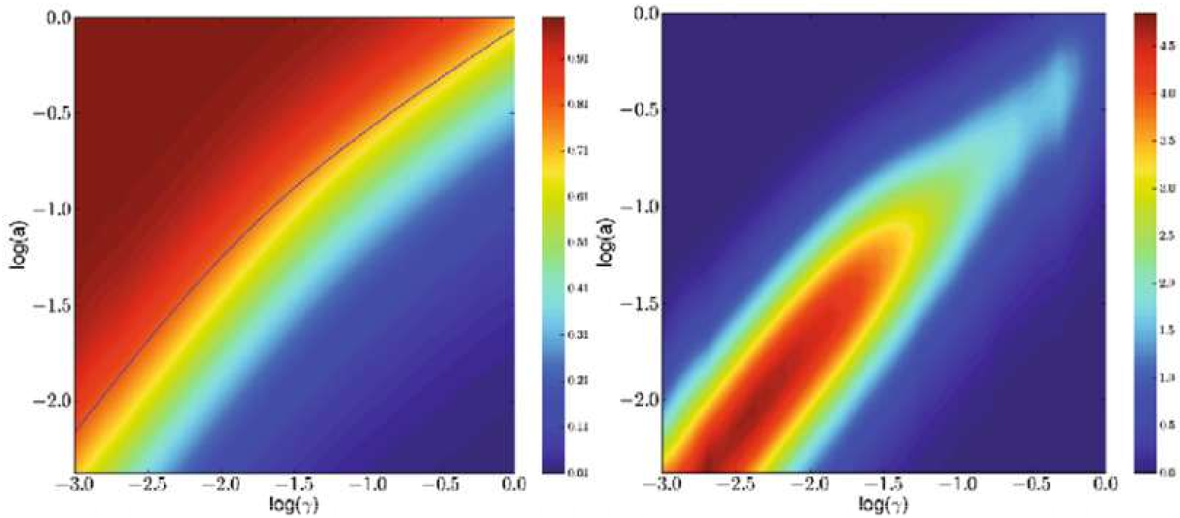

Fig. 10. (Color online) Dynamical correlation functions computed over the particles of sample containing 2500 particles and sheared at $\dot\gamma = 10^{-4}$ under RWBCs for a total strain $\epsilon_{\rm tot} = 200\%$. Left: correlation function $Q_s(a,\gamma)$ as a function of the probing length a and the strain γ in a log-log colormap. Right: four-point correlation function $\chi_4(a,\gamma)$ in a log-log colormap.

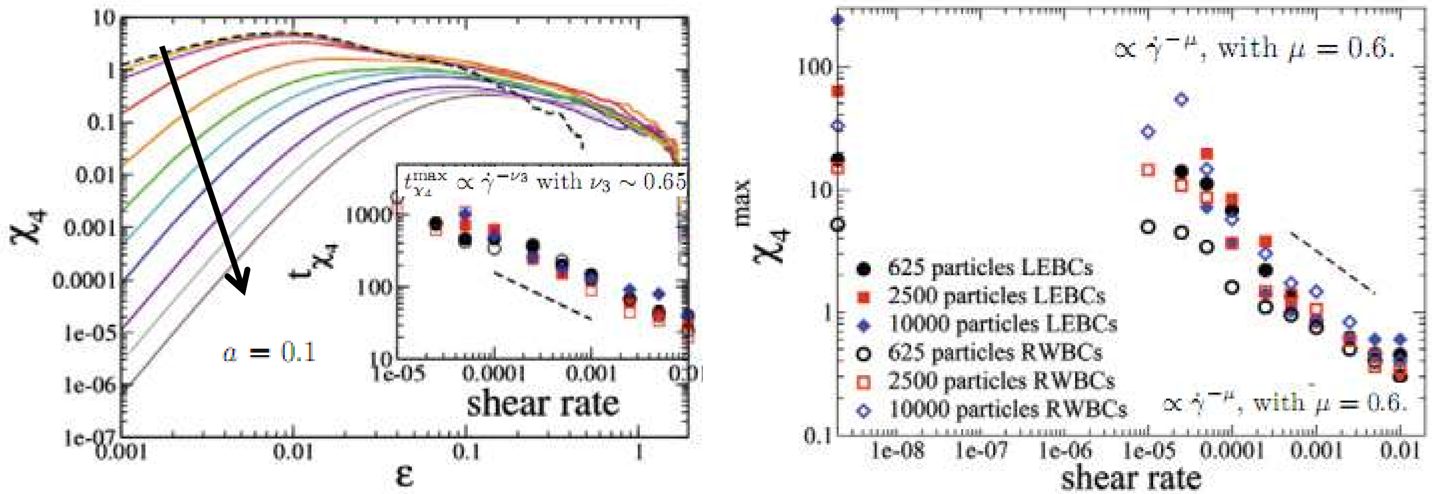

Dynamical Heterogeneities:

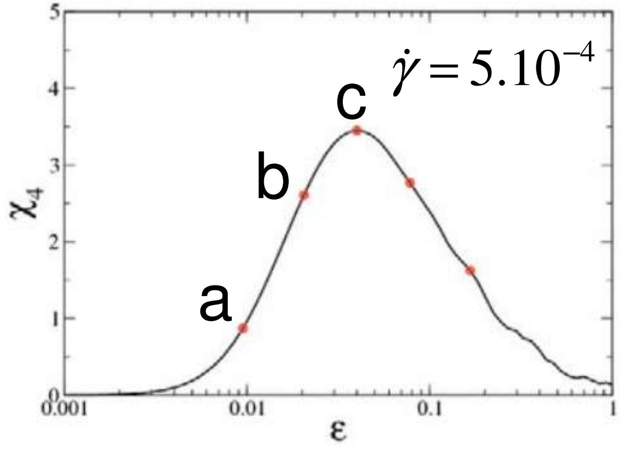

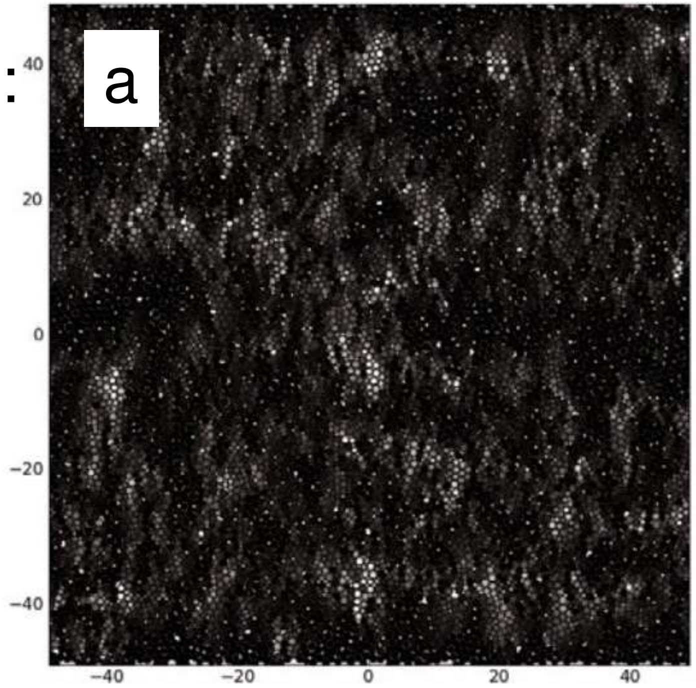

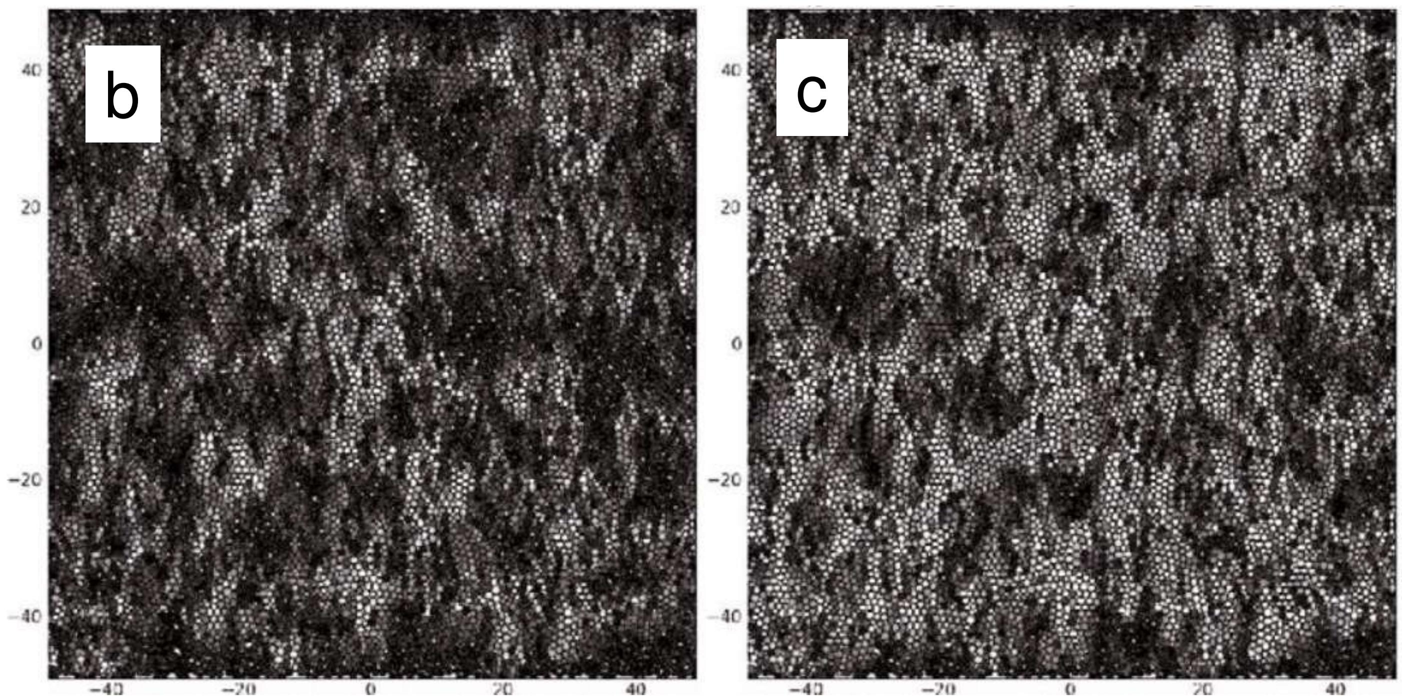

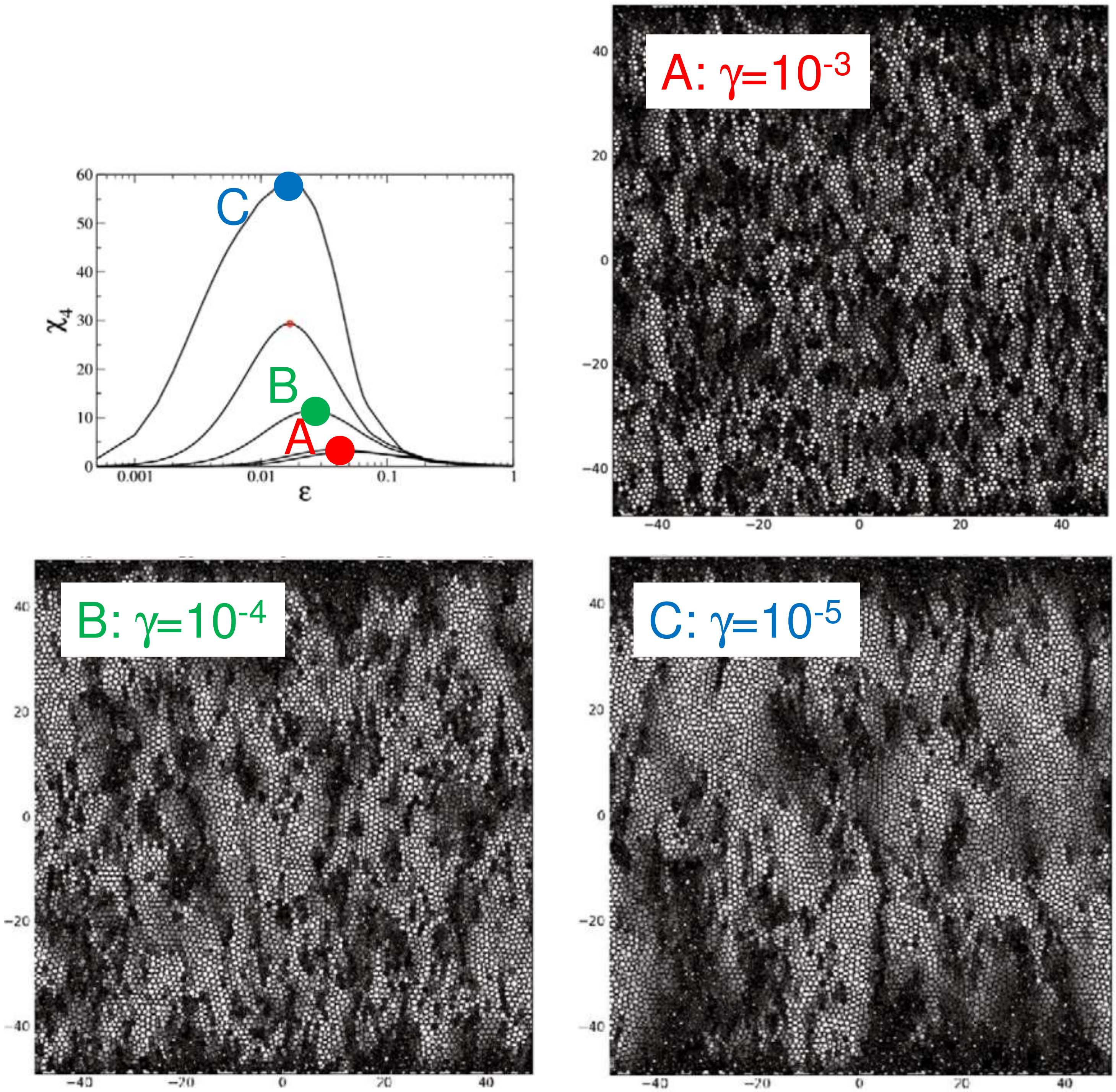

A: $\gamma=10^{-3}$
B: $\gamma=10^{-4}$
C: $\gamma=10^{-5}$
χ_4
ε
A
B
C

III. **Computation of Mechanical Quantities**

stress, strain, Elastic Moduli
identification of plastic rearrangements

Calculation of local elastic moduli from coarse-grained (continuous) fields:

displc[ts] $\mathbf{U}^{\mathrm{lin}}(\mathbf{R},t) = \frac{\sum_i m_i u_{i\alpha}(t)\phi[\mathbf{R}-\mathbf{r}_i(t)]}{\sum_j m_j \phi[\mathbf{R}-\mathbf{r}_j(t)]} + \mathcal{O}(\epsilon^2)$ with $\phi(\mathbf{r}) = \frac{1}{\pi w^2} e^{-(|\mathbf{r}|/w)^2}$

stress $\sigma_{\alpha\beta}(\mathbf{r},t) = -\frac{1}{2}\sum_{ij;i\neq j} f_{ij\alpha} r_{ij\beta} \overbrace{\int_0^1 ds\,\phi[\mathbf{r}-\mathbf{r}_i(t)+s\mathbf{r}_{ij}(t)]}^{=\phi[\mathbf{r}-\mathbf{r}_i(t)]+\mathcal{O}(|\mathbf{r}_{ij}|/w)}$ "contact stress"

2D case:

$$\begin{pmatrix} \delta\sigma_{xx} \\ \delta\sigma_{yy} \\ \sqrt{2}\delta\sigma_{xy} \end{pmatrix} = \begin{pmatrix} \hat{C}_{xxxx} & \hat{C}_{xxyy} & \hat{C}_{xxxy} \\ \hat{C}_{xxyy} & \hat{C}_{yyyy} & \hat{C}_{yyxy} \\ \hat{C}_{xxxy} & \hat{C}_{yyxy} & \hat{C}_{xyxy} \end{pmatrix} \begin{pmatrix} \epsilon_{xx} \\ \epsilon_{yy} \\ \sqrt{2}\epsilon_{xy} \end{pmatrix}$$

- Isotropic case:

$$\hat{C} = \begin{pmatrix} \lambda+2\mu & \lambda & 0 \\ \lambda & \lambda+2\mu & 0 \\ 0 & 0 & 2\mu \end{pmatrix} \Rightarrow \begin{array}{l} \Lambda_1 = \Lambda_2 = 2\mu \\ \Lambda_3 = 2(\lambda+\mu) \end{array}$$

6 unknowns $C_{\alpha\beta\gamma\delta}$ obtained through 3 independent sollicitations (**9 eq.**)

Maps of **local** elastic moduli:

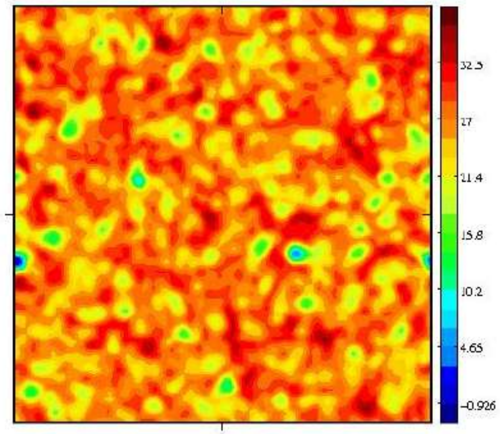

$C_1 \sim 2\ \mu_1$

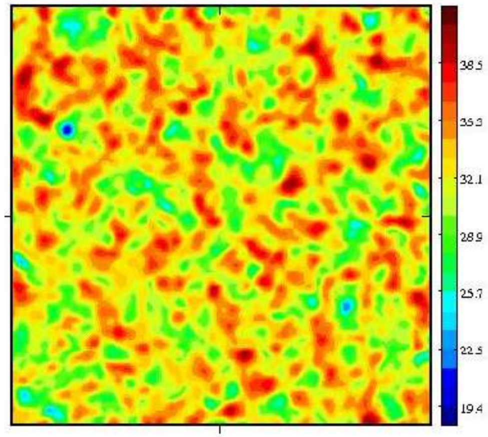

$C_2 \sim 2\ \mu_2$

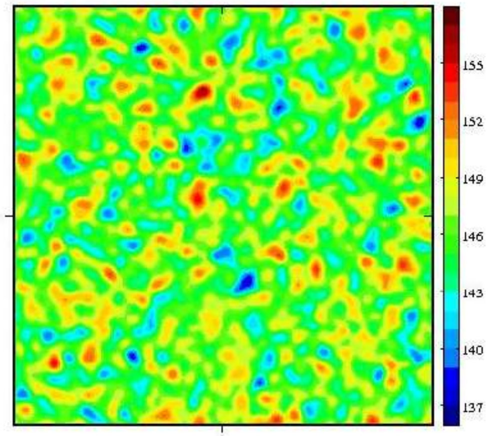

$C_3 \sim 2\ (\lambda+\mu)$

2D Jennard-Jones N = 216 225 L = 483 a

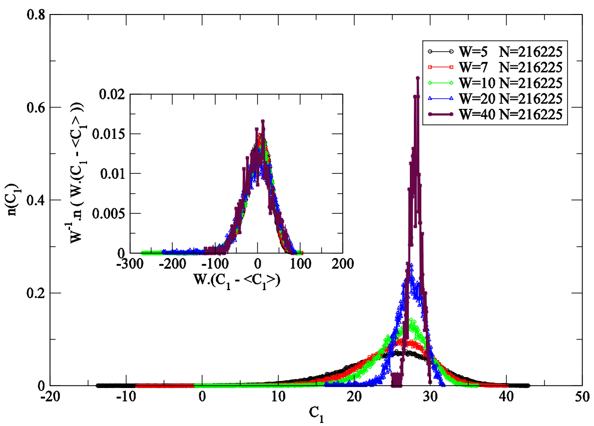

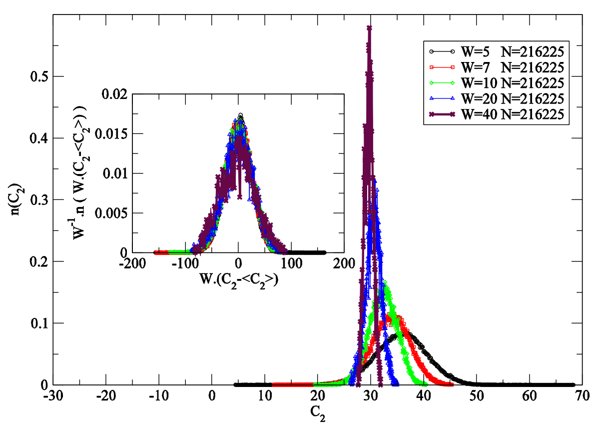

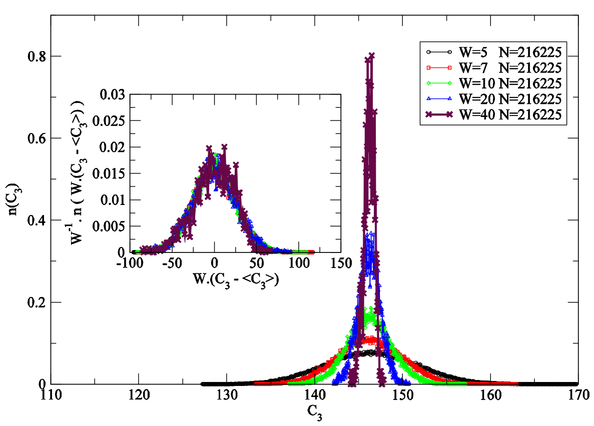

$$\Delta C \propto \langle C \rangle - C_\infty \propto \frac{1}{W}$$

Large scale convergence to **homogeneous** and **isotropic** elasticity

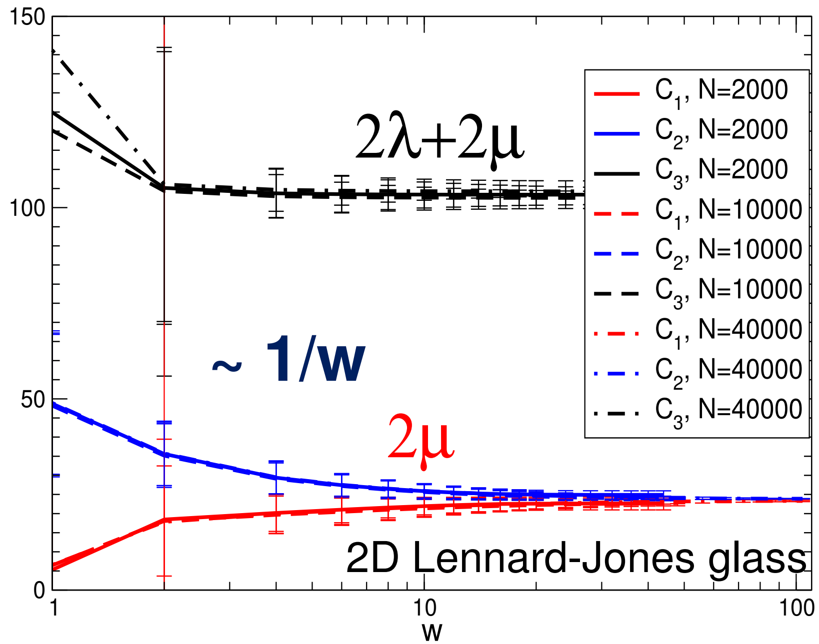

$$\text{Error: } \Delta = \frac{\left|\underline{\underline{\sigma}}_{\text{computed}} - \underline{\underline{\sigma}}_{\text{measured}}\right|}{\left|\underline{\underline{\sigma}}_{\text{measured}}\right|}$$

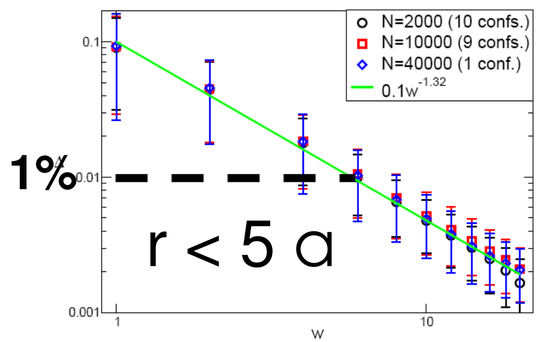

Coarse Graining

Linear Elasticity

W	0	5	10	15	20 a
Hooke's law	NO	YES	YES	YES	YES
Homogeneity $\frac{\langle c\rangle(W)-2\mu}{2\mu}<10\%$	NO	NO	YES	YES	YES
$\frac{\Delta C}{\langle c\rangle}<10\%$	NO	NO	NO	YES	YES
Isotropy $\frac{c_2-c_1}{2\mu}<10\%$	NO	NO	NO	NO	YES

Isotropic Elasticity

M. Tsamados et al. EPJE (2009)

Evolution of the Elastic Moduli during plastic deformation:

Modulus C_1(W=5a) during plastic deformation:

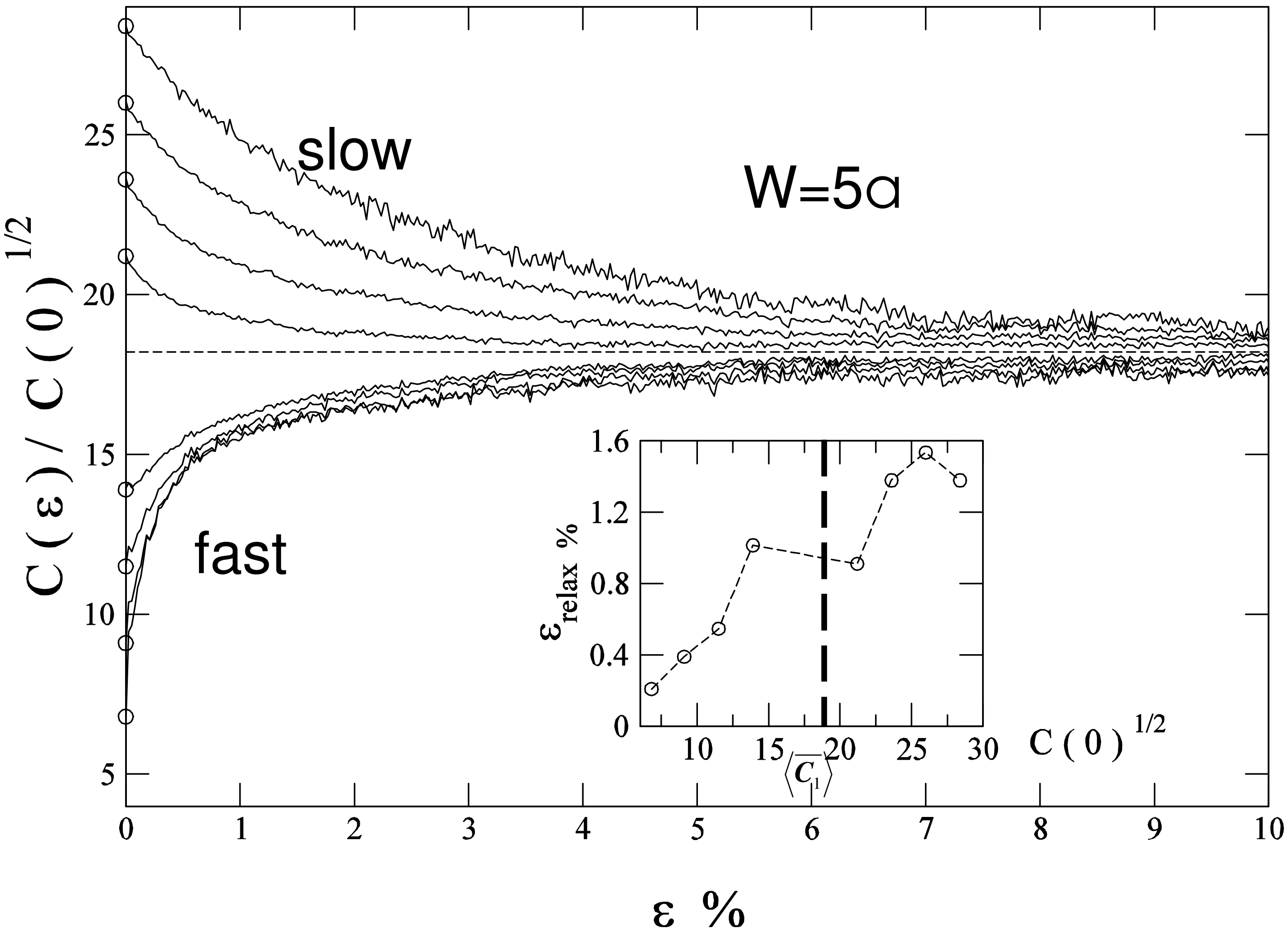

Splitting of the system into ***rigids*** ($C_1 > \langle \overline{C_1} \rangle$) and ***softs*** zones ($C_1 < \langle \overline{C_1} \rangle$).

Shear Banding as a *Percolation* of *Soft* Zones:

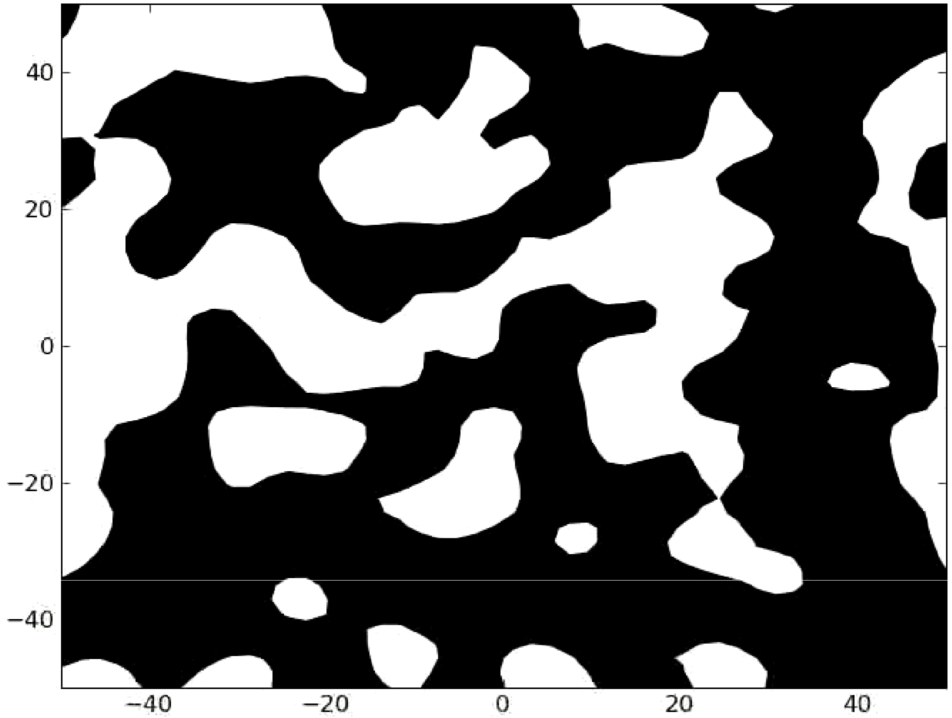

White: $c_1 < \langle \overline{C_1} \rangle$
Black: $c_1 > \langle \overline{C_1} \rangle$

M. Tsamados et al.
EPJE (2009)

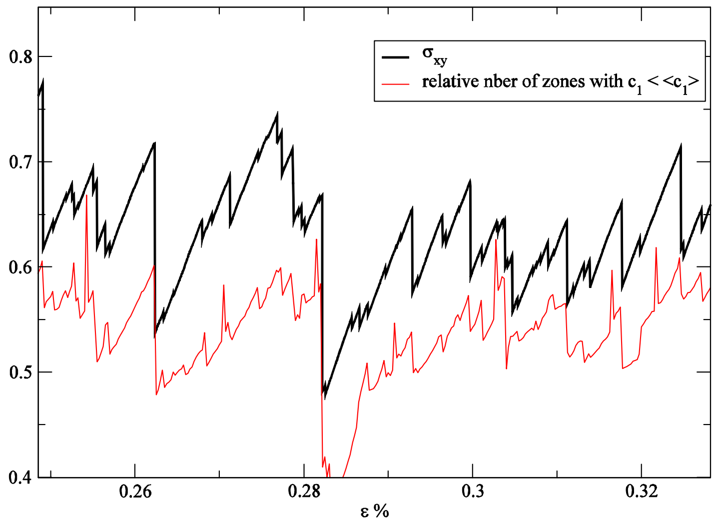

The proportion of *soft* zones evolves in parallel with the *total stress*.

Percolation before Shear Bands

Local event:

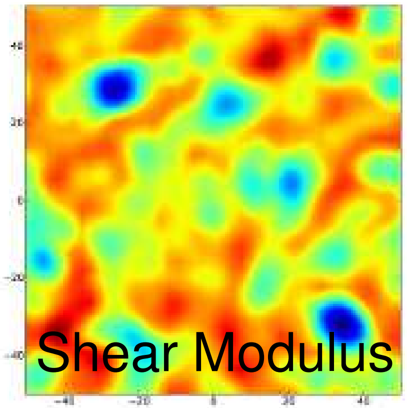

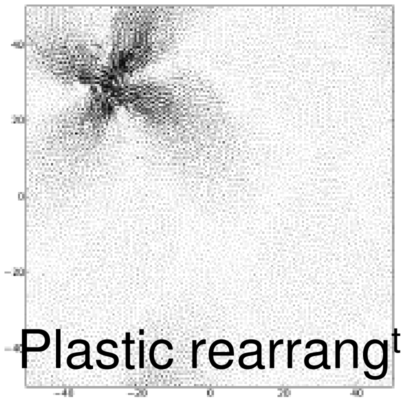

Elementary shear band:

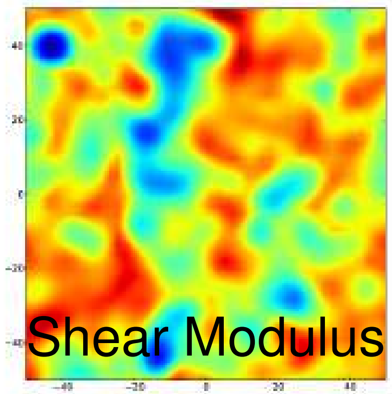

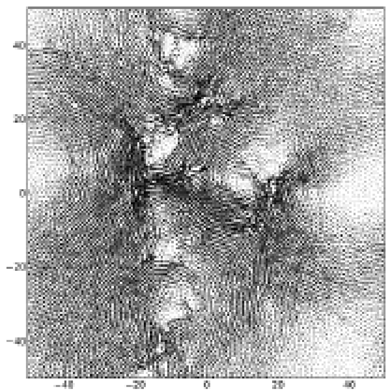

Percolation
before
Shear *Bands*

A. Tanguy and B. Mantisi EPL (2010)

Other order parameters:

Modulus C_1

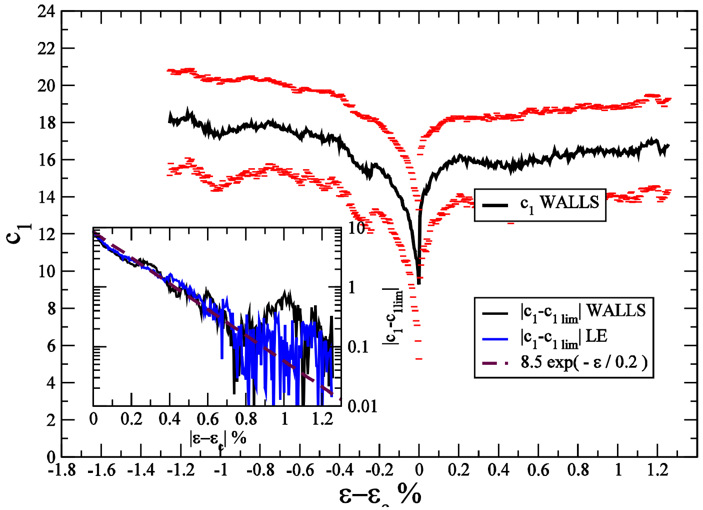

Shear stress σ_{xy}

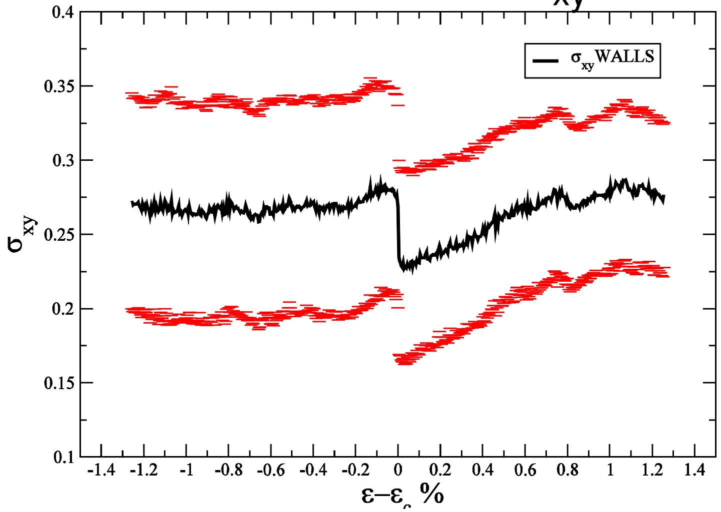

Mass density:

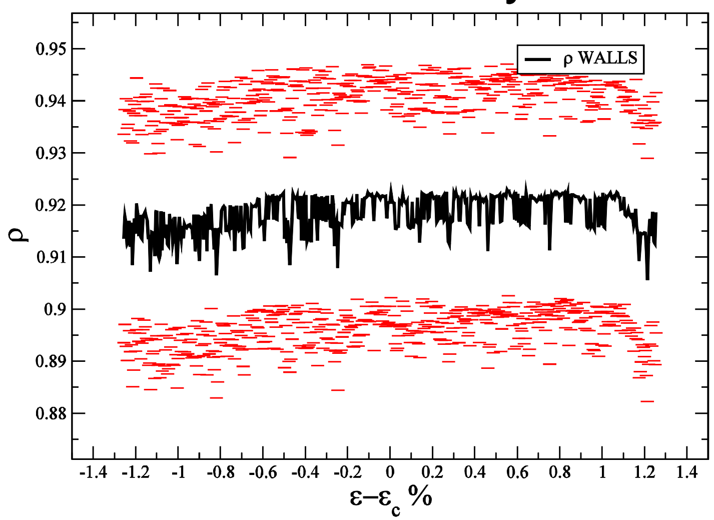

Coordination number:

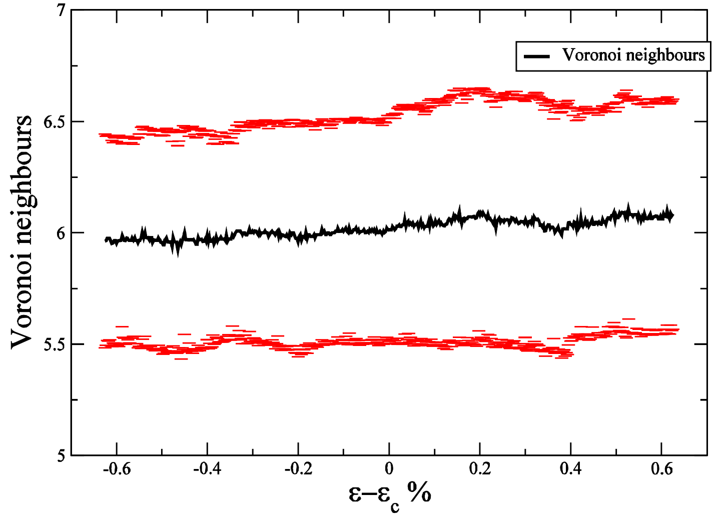

The lowest Local *modulus* C1 allows to anticipate *plastic activity*.

Vibrational Properties:
The role of Local Elastic Moduli ?

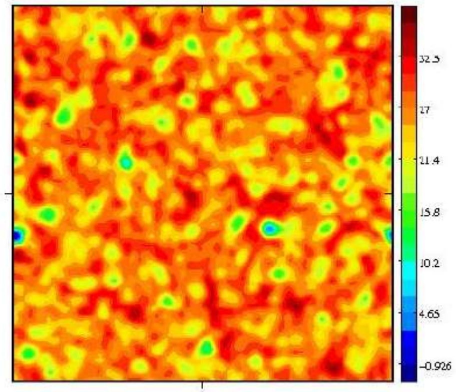

$C_1 \sim 2\,\mu_1$

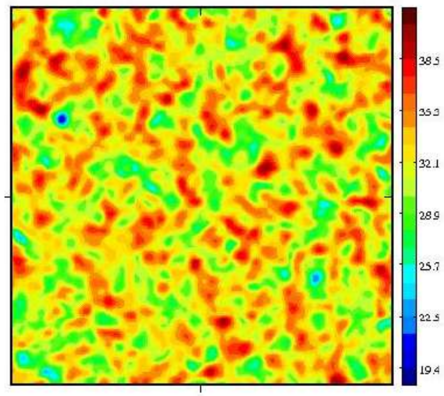

$C_2 \sim 2\,\mu_2$

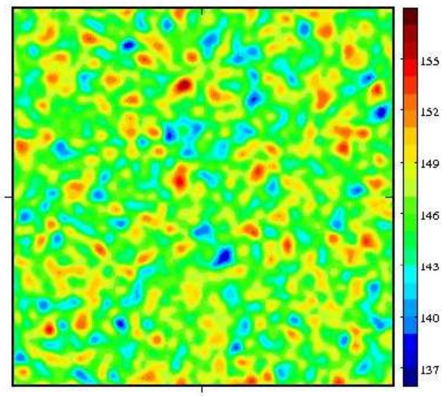

$C_3 \sim 2\,(\lambda+\mu)$

Verre modèle de LJ   N=216 225   L=483

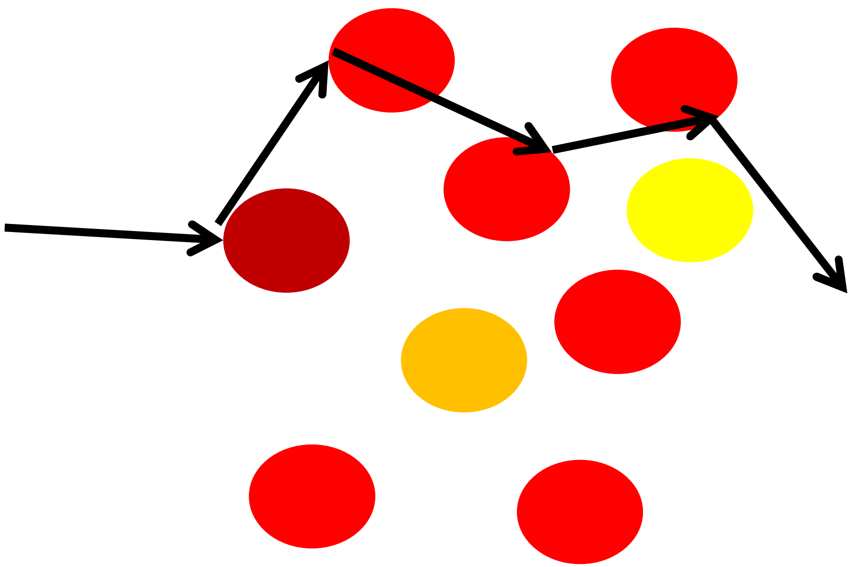

$$\rho \frac{\partial^2 \underline{u}}{\partial t^2}(\underline{r}) = \nabla.(\underline{\underline{\underline{\underline{C}}}}(x,y,z):\underline{\underline{\varepsilon}}) + \underline{f}$$

4 possibilities:

- **Coherent propagation**
- **Low scattering** (Rayleigh)
- **Strong scattering**
- **Localisation** (Ioffe-Regel)

Exact Diagonalization of the Dynamical Matrix:

Moduli and Eigenfrequencies:

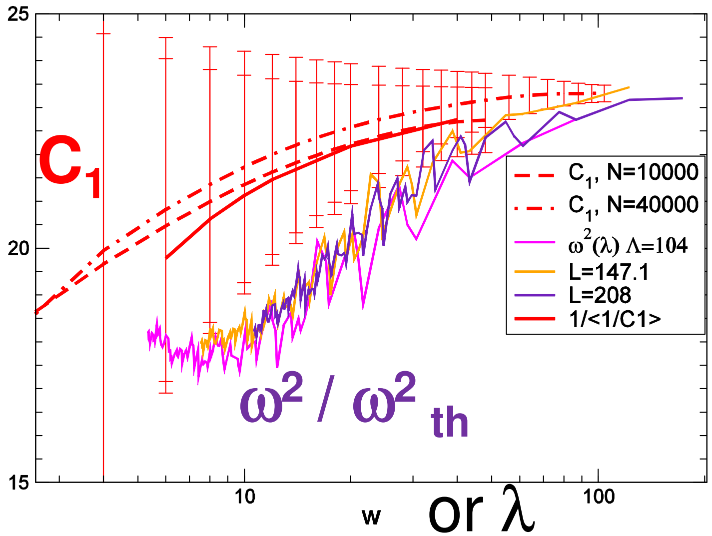

$\omega^2_{th} \sim C_{1\infty}/\lambda$

Density of vibrational states:

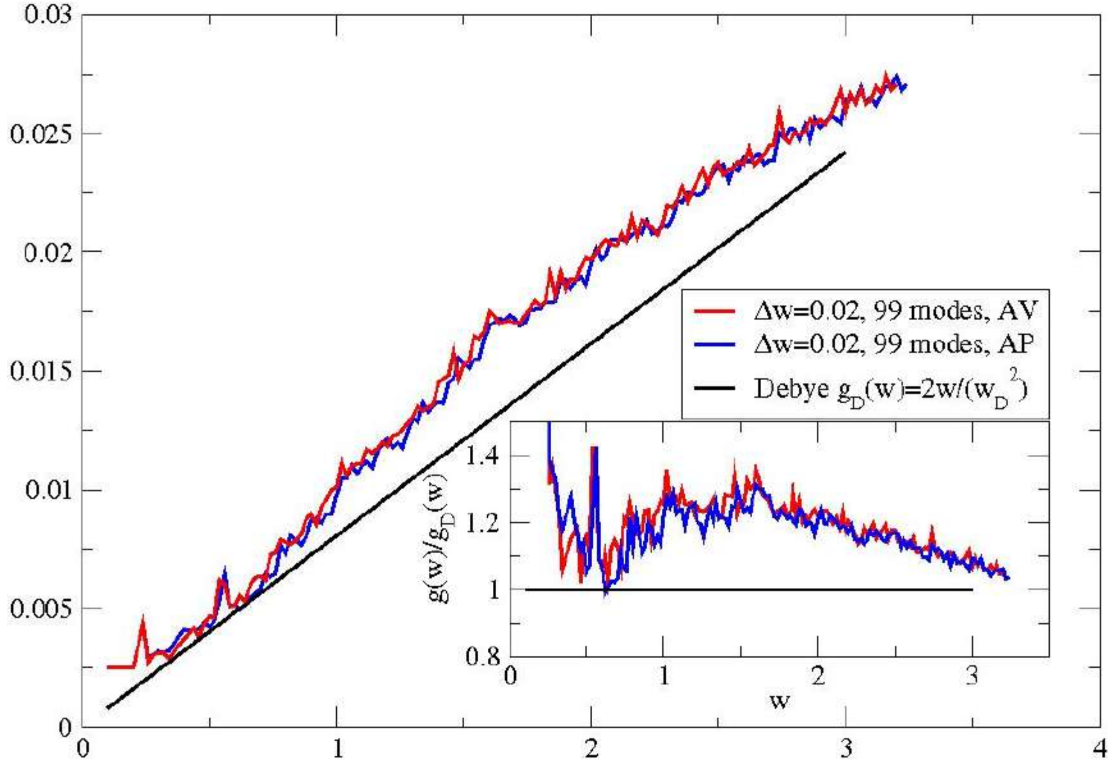

2D Lennard-Jones system,
Boson Peak

A. Tanguy (2002) S. Mossa (2008) B. Mantisi (2010)

Projection of the vibration modes on the plane waves:

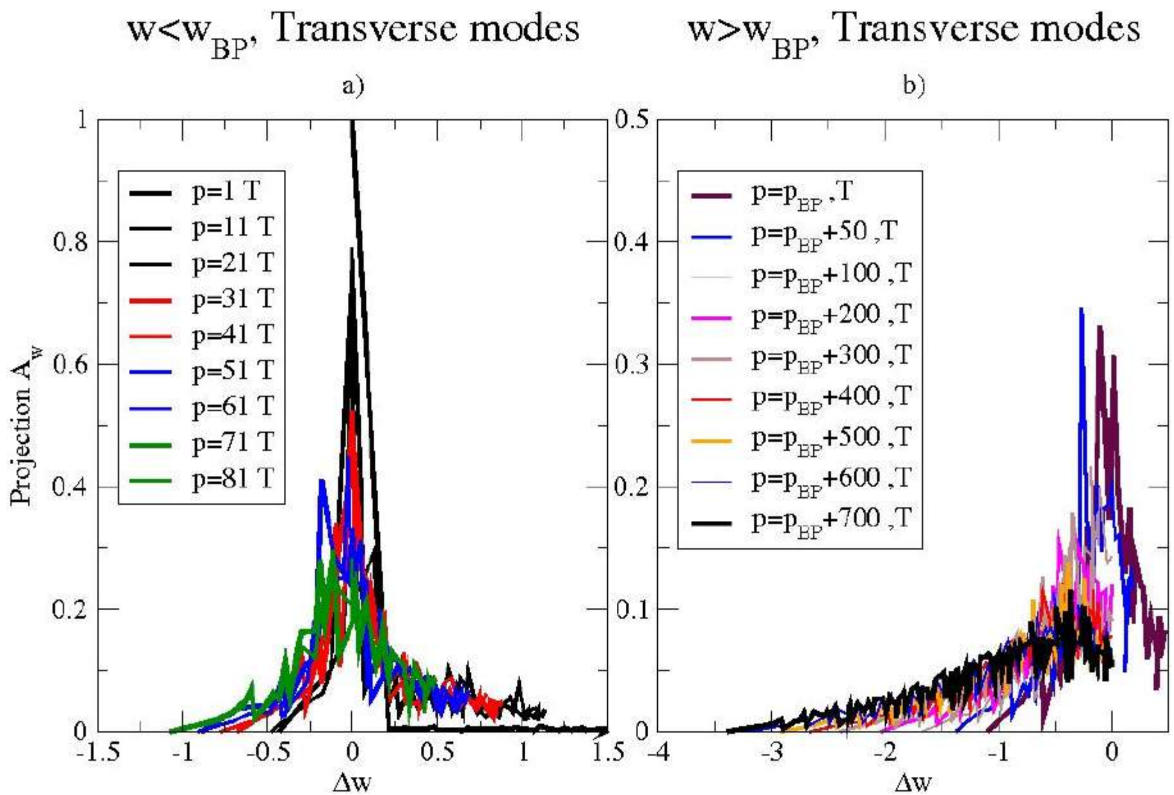

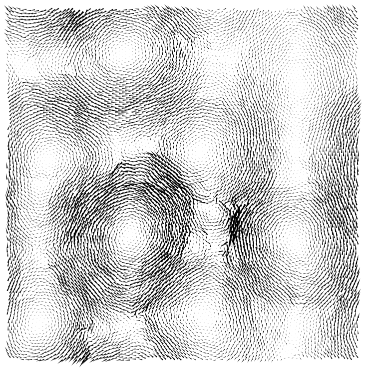

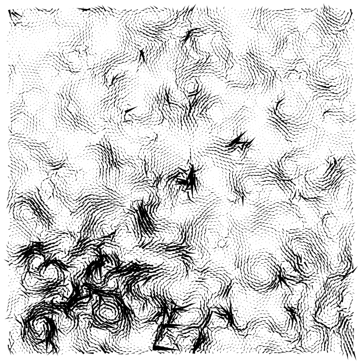

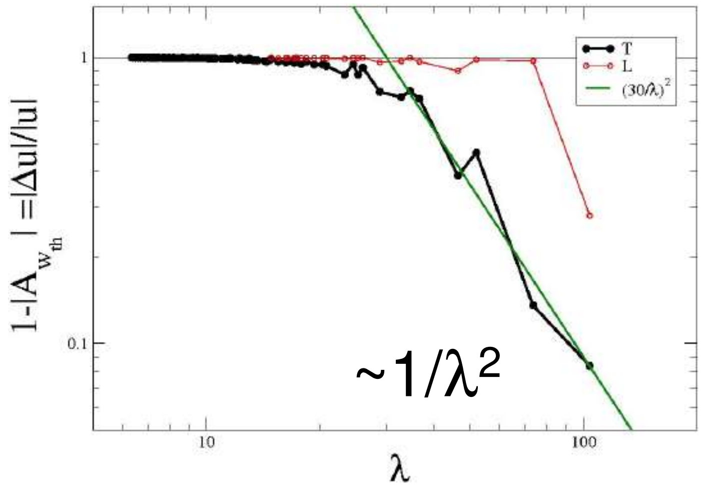

Rayleigh scattering

$\xi \sim 25\ a$

for $w < w_{BP}$

B. Mantisi (2010)

Proximity to a Plastic Rearrangement: Localization at low frequency

Vibration Modes,
Close to a Plastic Rearrangement?

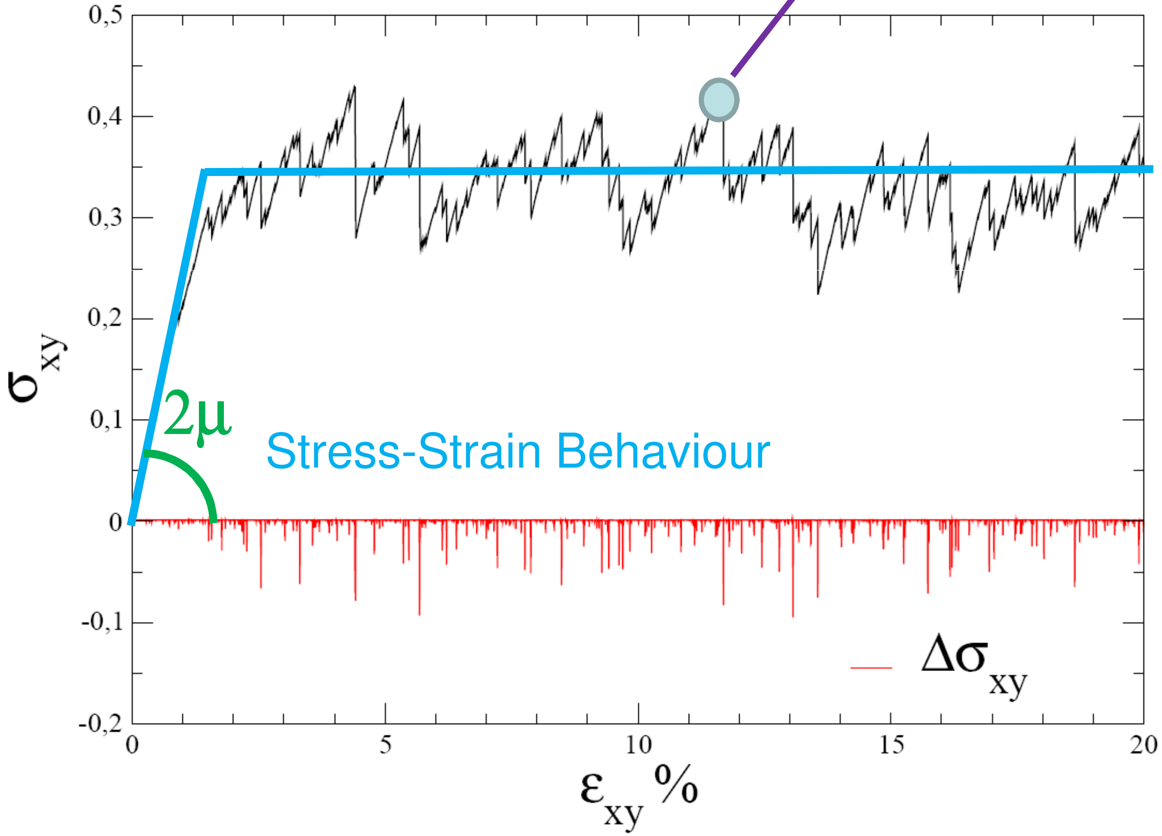

Tanguy,
Tsamados
(2007,2008)
Lemaître (2004)

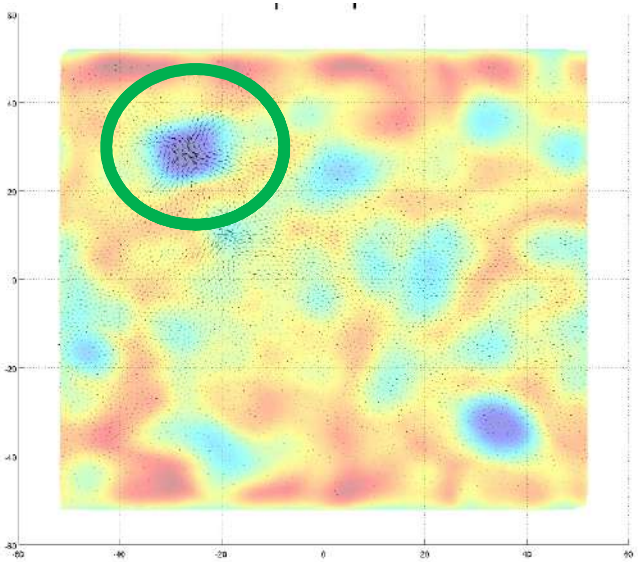

Local Shear Modulus

Eigenfrequenciess:

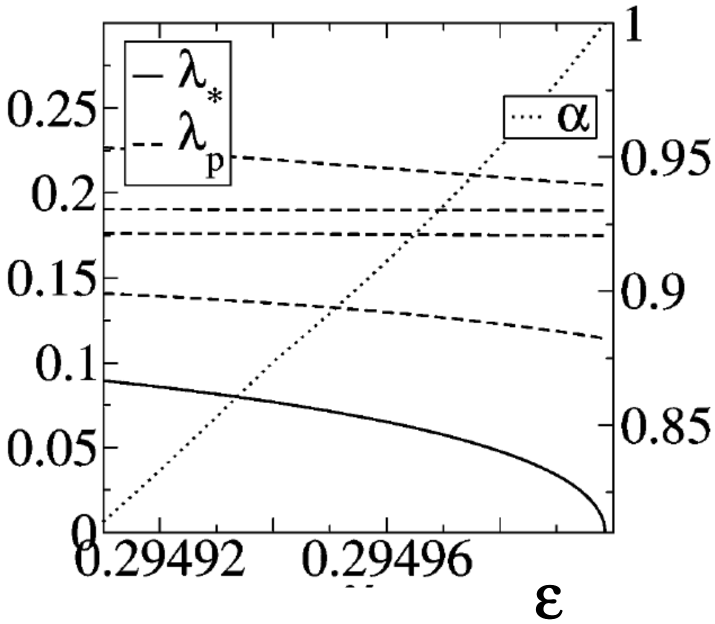

Plastic Rearrangement:

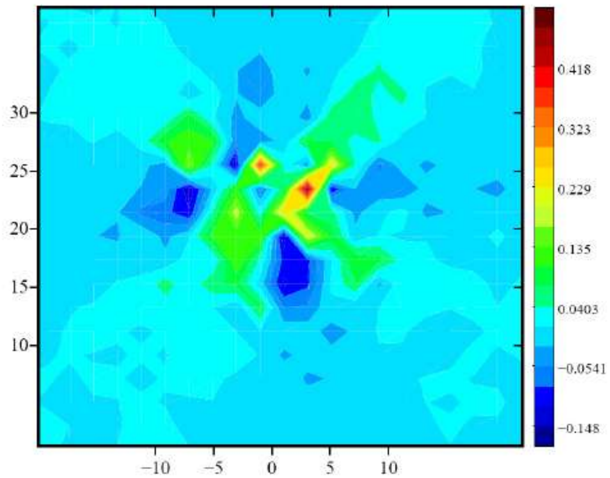

Localized vibration mode:

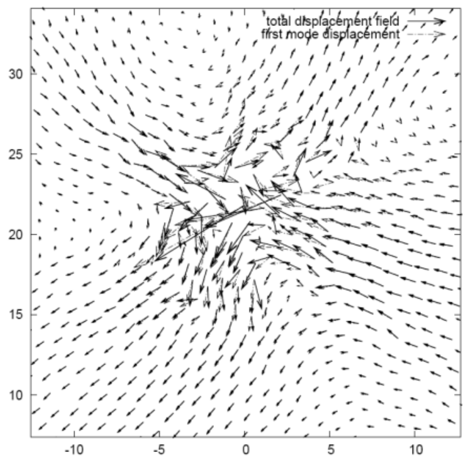

Localization on *Soft* zone
of *Low* Frequency vibration

Just before
a **plastic** rearrangement.

Local event:

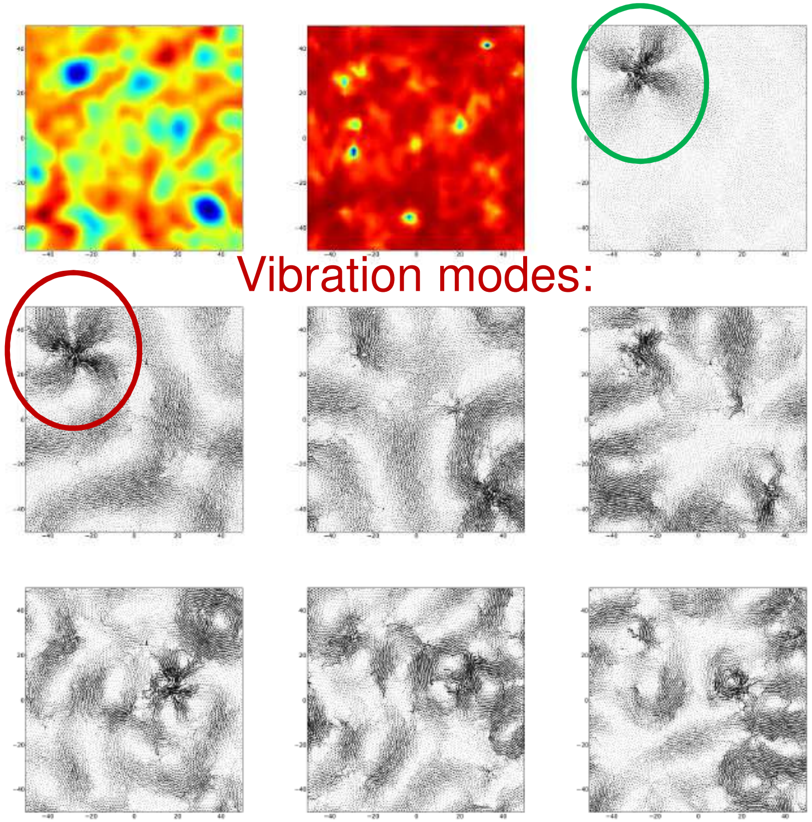

A single localized mode

Elementary shear band:

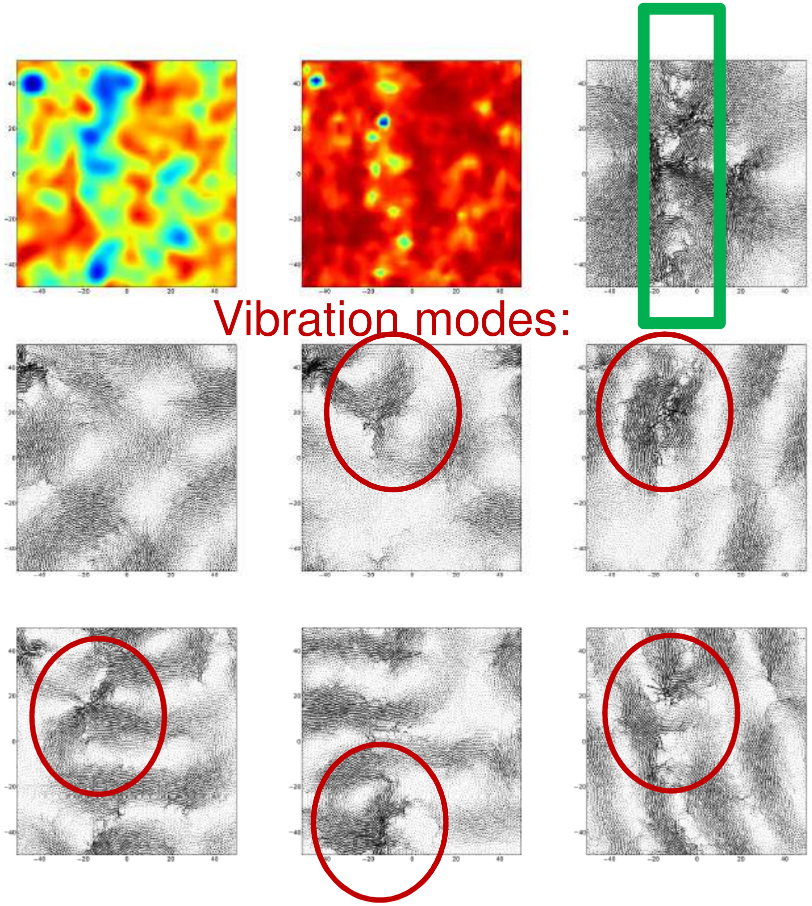

Superposition
of localized modes

Identification of Plastic Rearrangements

Determination of the size of the Plastic Events:

Size of the basins in the Local Plastic Energy Function

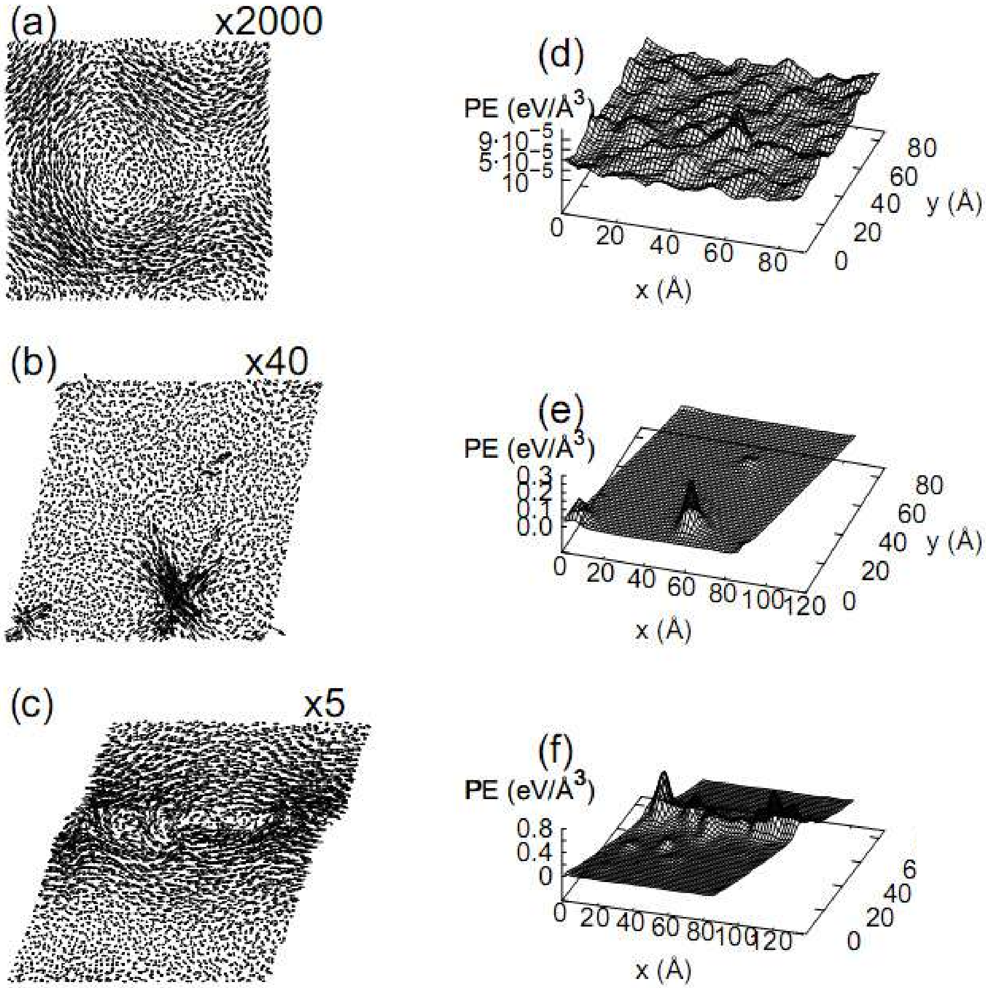

$$PE_{at}(i_a) = \left(\sum_{j_a} |V^{2b}_{i_a,j_a}(\epsilon_i^{ini}) - V^{2b}_{i_a,j_a}(\epsilon_i^{rev})|^2 + \sum_{j_a}\sum_{k_a} |V^{3b}_{j_a,i_a,k_a}(\epsilon_i^{ini}) - V^{3b}_{j_a,i_a,k_a}(\epsilon_i^{rev})|^2 \right)^{1/2}$$

$$PE(r) = \sum_{i_a} PE_{at}(i_a)\left(\frac{1}{(\pi\omega^2)^{3/2}} \exp - \frac{|r - r_{i_a}|^2}{\omega^2}\right)$$

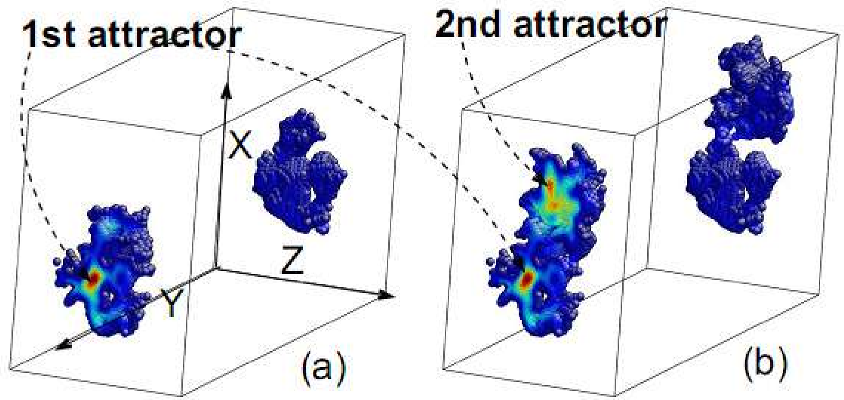

Example of « a-silicon »

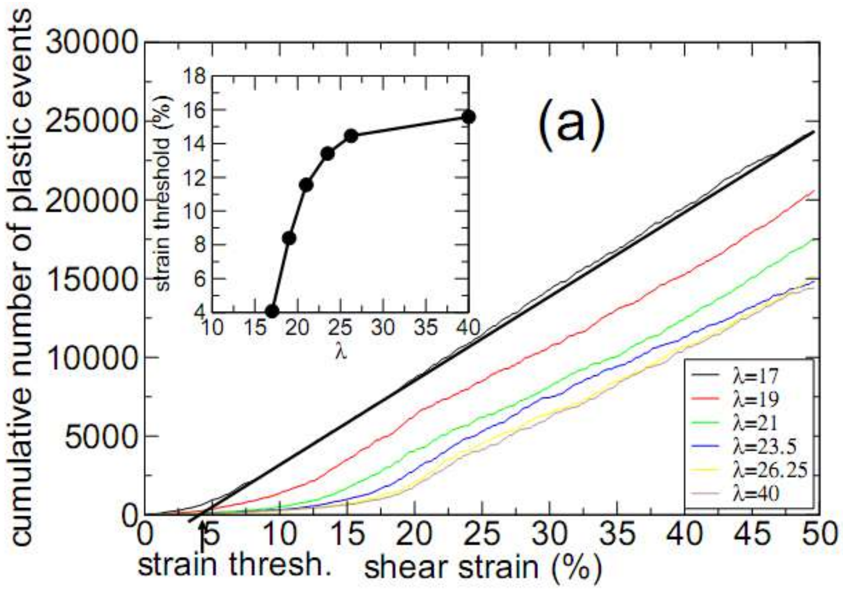

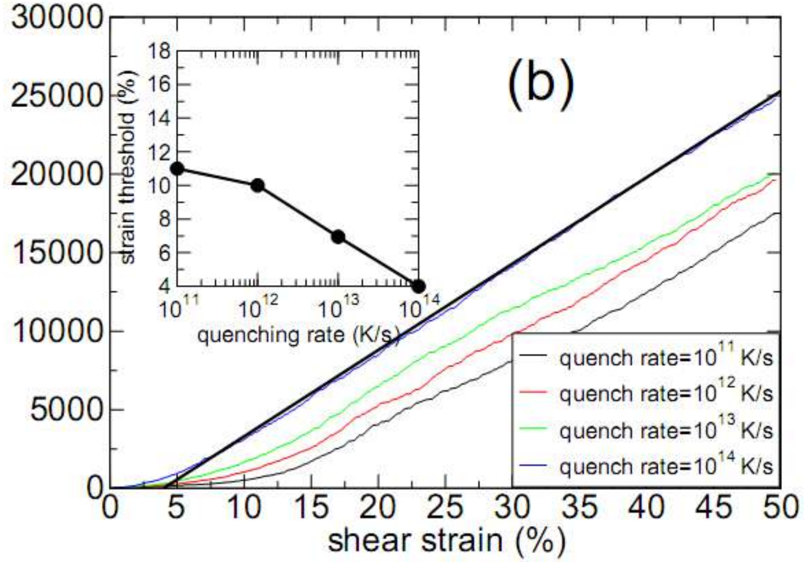

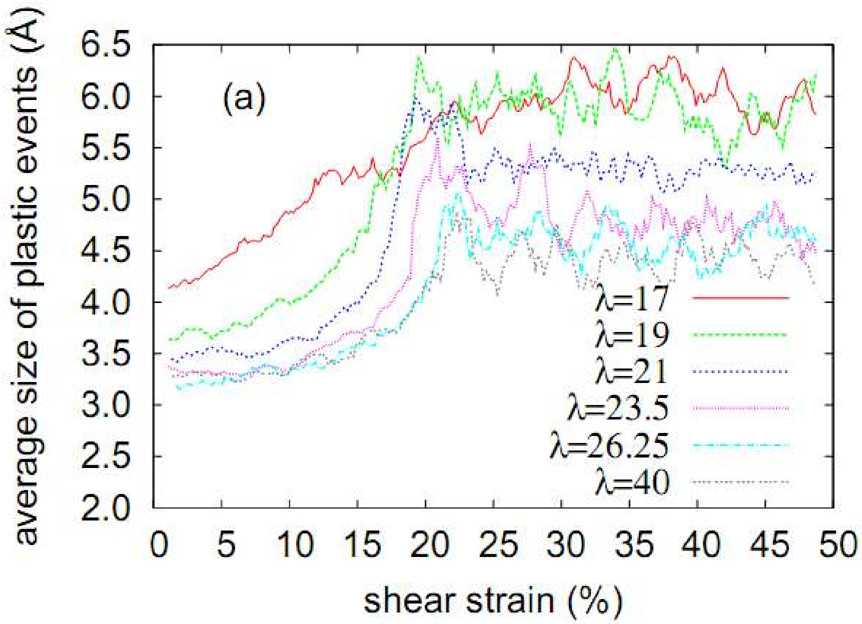

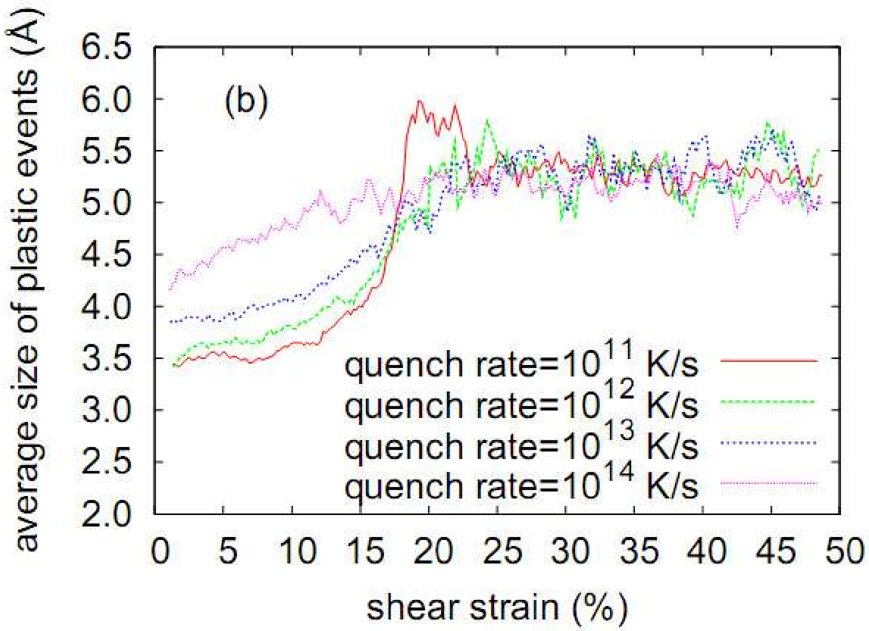

The Peierls stress

$$\boxed{\sigma^*_{xy} = Ae^{-2\pi W/b}}$$

where $A = 2C_{44}/(1-\nu)$

$b \approx 1.6\ \text{Å}$

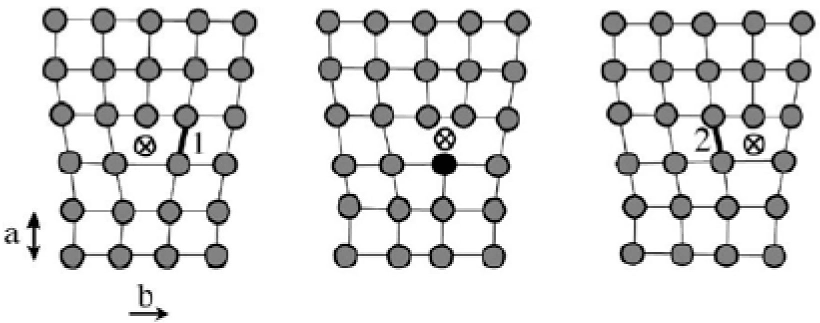

TABLE III: Yield stresses σ_Y, width of the plastic event at the yield point W and corresponding values of b obtained by using Eq. (5) for different values of λ for a A-Si system prepared with a quenching rate of 10^{11} K/s, and for different values of the quenching rate at $\lambda = 21$.

λ	ν	W (Å)	σ_Y(GPa)	b (Å)
17	0.389	6.11	2.01	1.64
19	0.365	6.11	2.80	1.75
21	0.347	5.63	4.23	1.75
23.5	0.331	5.13	5.47	1.67
26.25	0.318	4.73	6.64	1.59
40	0.273	4.57	10.13	1.59
quench. rate		W (Å)	σ_Y (GPa)	b (Å)
10^{11} K/s		5.63	4.23	1.75
10^{12} K/s		5.39	3.53	1.61
10^{13} K/s		5.39	3.0	1.56
10^{14} K/s		5.30	2.32	1.45

Strong dependence of the **size** of the plastic events on λ.

Analogy with *dislocation's width* in crystals.

Role of Local Coordination Defects:

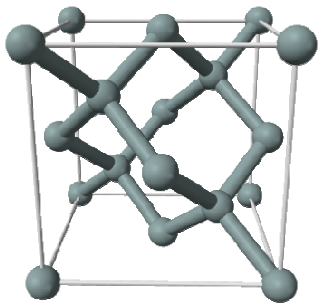

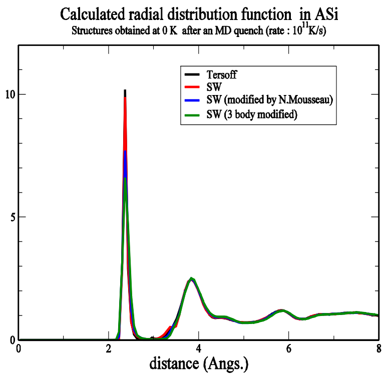

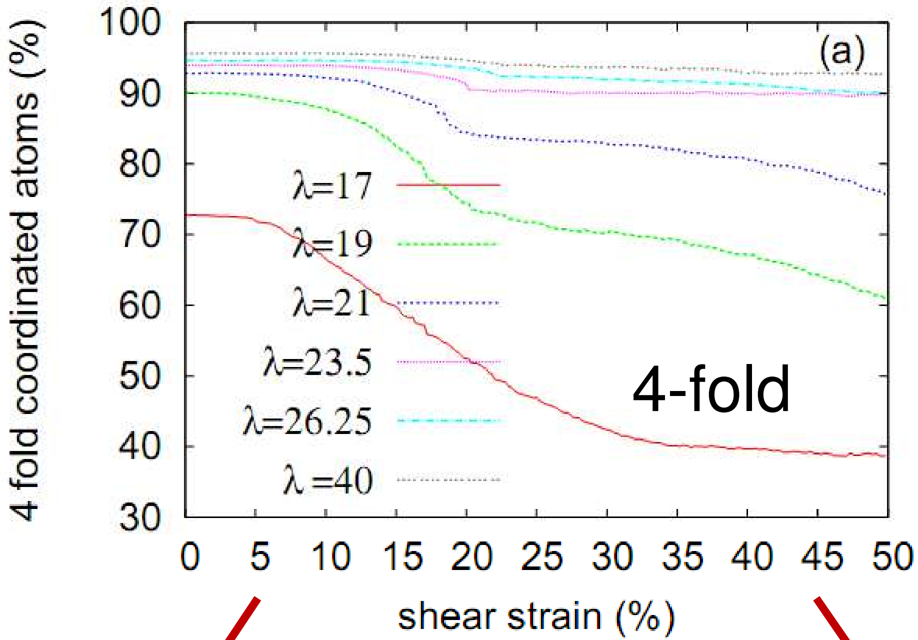

The **type** and the **number** of defects depends strongly on λ.

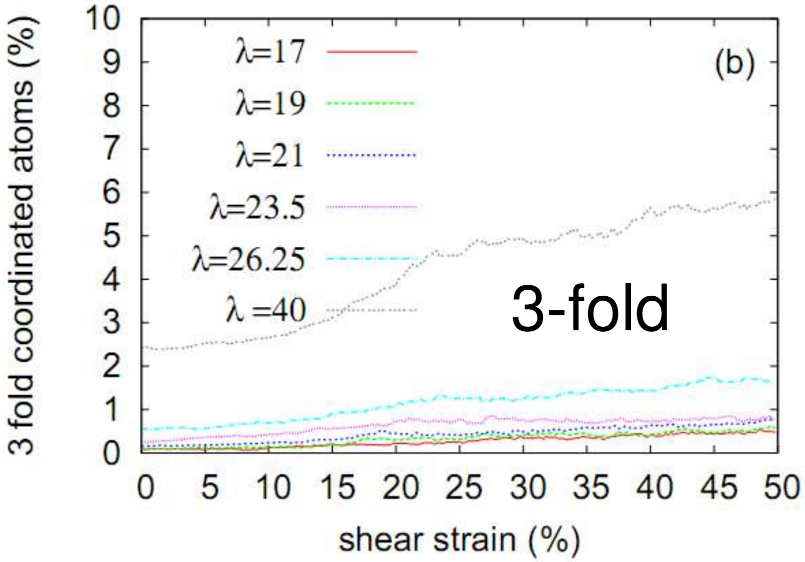

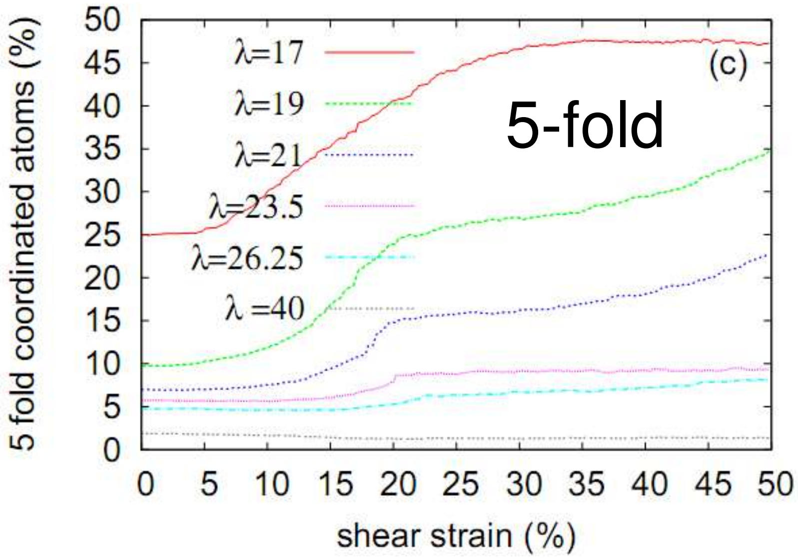

Connection between plastic events and defects:
as a function of the 3-body interaction λ

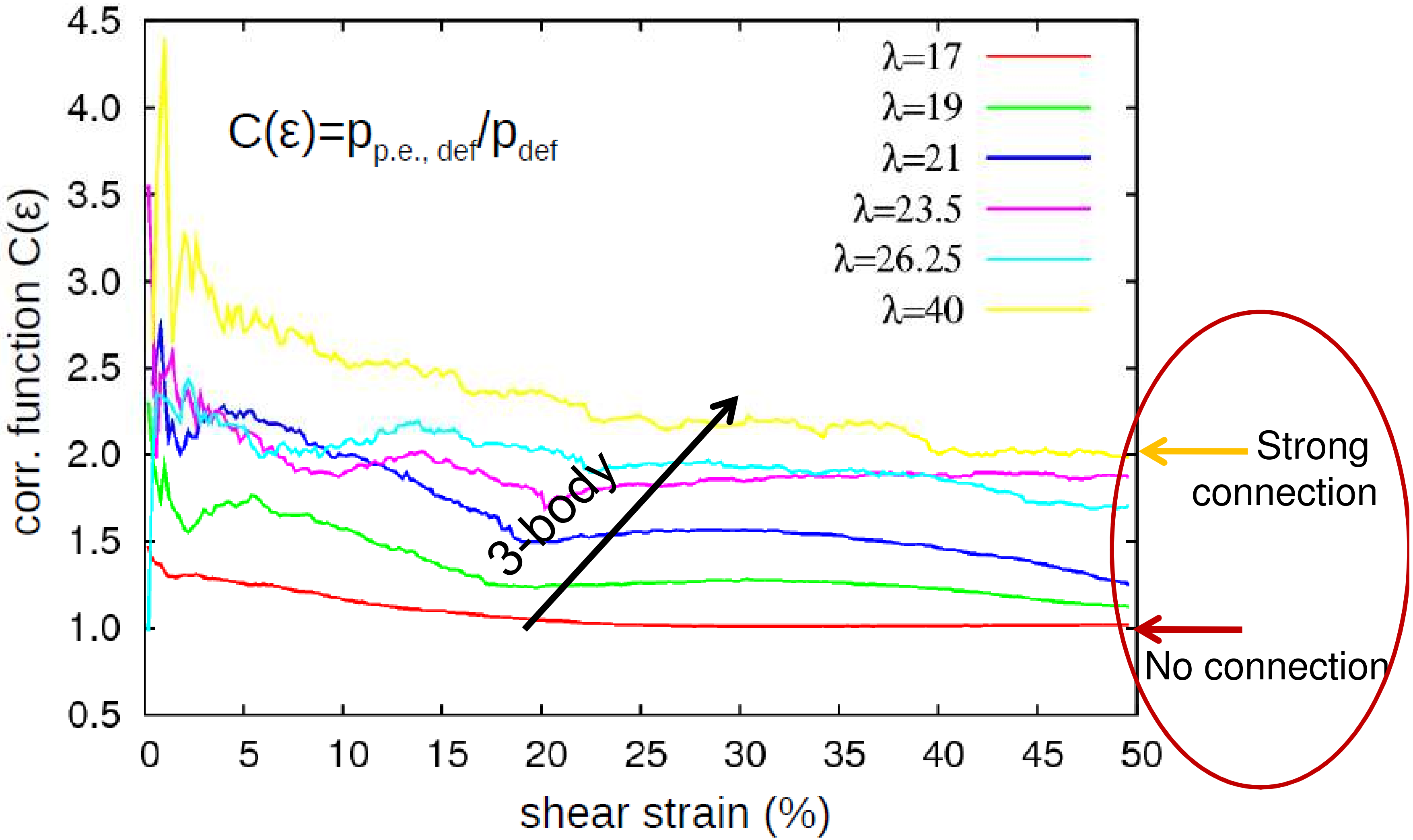

The connection to the **local coordination defects** depends on the strength of the *3-body* interaction

C. Fusco et al. (2010)

Conclusion

Length Scales ~ 3 nm
Time Scales ~ 10 ns or **Quasi-Static** athermal simulations
Role and description of the **Temperature**? Athermal regime?

Universal phenomenology of plasticity in glasses:
Quadrupolar Events and **Shear Bands** ~**nm** scale

The **Local Bound Directionality** affects:
The **Width** of the Plastic Event (**Peierls Stress**)
The **number**, the **type** of coordination defects and their **evolution** upon external strain
The **connection** between plastic events and Local coordination defects

Competition between **shear** and **densification** in **Silica-like Glasses**:
The pressure hardening favors a more **homogeneous** atomistic response

The **Dynamical Evolution** of the **Local Elastic Moduli** is directly connected
to the **plastic Behaviour** in Lennard-Jones systems.
Its **heterogeneity** gives rise to **low scattering of acoustic waves** at low frequencies.
The **dynamical evolution** of the Elastic Moduli is related to a **significative change**
of the **very low frequency Acoustic Modes** close to a **plastic rearrangement**.